Geometries and slip of historical surface-rupturing earthquakes in New Zealand and their application to seismic hazard analysis

Andy Nicol, Narges Khajavi, Jade Humphrey, Russ Van Dissen, Matt Gerstenberger, Mark Stirling

Geometries and slip of historical surface-rupturing earthquakes in New Zealand and their application to seismic hazard analysis

Principal Investigator: Andy Nicol, University of Canterbury

Research team: Narges Khajavi, University of Canterbury

Jade Humphrey, University of Canterbury

Russ Van Dissen, GNS Science

Matt Gerstenberger, GNS Science

Mark Stirling, University of Otago

Date: May 2022

Non-technical summary

This project was conceived prior to the 2016 Kaikōura Earthquake after recognising that many of New Zealand's historical earthquakes produced displacement on interconnected networks of active faults (e.g., 1987 Edgecumbe and 2010 Darfield earthquakes). The Kaikōura Earthquake ruptured at least 17 separate faults and reminded the global earthquake community of the potential for large earthquakes to break more than one fault. It is clear from the Kaikōura Earthquake that such ruptures can be complicated, however, questions remain about how frequently they occur, what controls these multiple-fault earthquakes and whether we should expect similarly complex faulting patterns in future earthquakes? To address these questions we have reanalysed the literature and digital elevation models of the ground-surface for eight moderate to great historical earthquakes (magnitudes 6.4-8.2) in New Zealand since 1840. Of these earthquakes, at least five involved three or more faults (Wairarapa 1855, Hawkes Bay 1931, Edgecumbe 1987, Darfield 2010 and Kaikōura 2016 earthquakes). It is clear from the available information that earthquakes rupturing multiple faults have been common in New Zealand in the last ~180 years. These multiple fault ruptures occur on a range of fault types, with variable fault displacement rates and in different geological settings. Despite these differences, the relationship between average displacement of the ground surface and the rupture length appears to be mainly controlled by the dimensions of each individual fault plane and not by the size of the earthquake or the total number of faults that it ruptured.

For all historical multiple-fault earthquakes in New Zealand, the individual fault surfaces are linked together. In the Wairarapa 1855, Hawkes Bay 1931 and Kaikōura 2016 earthquakes co-rupture of Hikurangi subduction thrust faults beneath eastern New Zealand, may have facilitated rupture of more than one fault at the ground surface. Other earthquakes were far-removed from the Hikurangi subduction system, which is unlikely to have directly contributed to the observed complexity of fault ruptures (e.g., Buller 1929, Edgecumbe 1987 and Darfield 2010 earthquakes). Fault interactions promoted by their intersections and crustal stresses, are inferred to be the primary controls on the rupture of more than one fault during each earthquake. Compared to one-fault one-earthquake seismic hazard models inclusion of significant numbers of multiple fault ruptures is expected to increase the magnitudes and decrease the frequency of earthquakes greater than magnitude seven in size. Further work is required to determine the circumstances where the inclusion of earthquakes that rupture multiple faults in the NSHM, will increase or decrease the overall seismic hazards in different parts of the country.

Technical summary

This project was conceived prior to the 2016 Kaikōura Earthquake following recognition that numerous New Zealand historical surface-rupturing earthquakes produced slip on interconnected networks of faults (e.g., moment magnitude Mw 6.4 1987 Edgecumbe and Mw 7.1 2010 Darfield earthquakes). The Kaikōura Earthquake ruptured at least 17 separate faults and reminded the global seismology community of the potential for large earthquakes to rupture multiple faults. It is clear from the Kaikōura Earthquake that such ruptures can be complex, however, questions remain about what controls these multiple-fault earthquakes (here referred to as multi-fault earthquakes), their frequency and whether we should expect similarly complex ruptures in future earthquakes? To address these questions we have collated information from the literature and reanalysed digital elevation models for eight moderate to great historical earthquakes (Mw 6.4-8.2) that ruptured the ground surface in New Zealand post 1840. Of these earthquakes at least five ruptured three or more faults (Wairarapa 1855, Hawkes Bay 1931, Edgecumbe 1987, Darfield 2010 and Kaikōura 2016 earthquakes), and show a strong time-dependence, with all but one of these earthquakes post-dating 1930. The prevalence of these multi-fault events over the last ~90 years may reflect the improving quality and quantity of the available data rather than a change in the style of surface-ruptures. Independent of these sampling biases it is clear that rupture of multiple faults during individual earthquakes were common in New Zealand during the last ~180 years. These multi-fault ruptures occur for a range of fault types (e.g., strike-slip, normal and reverse), with variable fault displacement rates and in different tectonic settings. The scaling relationships between average displacement and rupture length generally do not vary between the largest (primary) and smaller (secondary) faults, or with slip type, displacement rates and the geological setting. These scaling relations are mainly controlled by the dimensions of each individual fault and not by the size of the earthquake or the total number of faults that it ruptures.

For all multiple-fault earthquakes, the individual fault surfaces that ruptured intersect in three-dimensions. The Wairarapa 1855, Hawkes Bay 1931 and Kaikōura 2016 earthquakes may have co-ruptured the Hikurangi subduction thrust (or thrust faults splaying from the subduction interface), which facilitated (and linked) rupture of more than one fault in the upper crust. The Buller 1929, Edgecumbe 1987 and Darfield 2010 multi-fault earthquakes did not involve the Hikurangi subduction system, which is unlikely to have directly contributed to the observed complexity of rupture geometries. Fault interactions promoted by their intersections and crustal stresses (both static and dynamic) are inferred to be the primary controls on the development of earthquakes that rupture multi-faults. Multiple-fault ruptures were included on some of the major faults in the 2010 National Seismic Hazard Model (NSHM), and they have increased in number for the 2022 NSHM. Compared to one-fault one-earthquake models inclusion of significant numbers of multiple fault ruptures are expected to increase the magnitudes and decrease the frequency of earthquakes greater than magnitude seven in size. Further work is required to determine under what circumstances the inclusion of multi-fault ruptures in the NSHM will increase or decrease overall seismic hazards.

Key words: Historical earthquakes, multi-fault ruptures, New Zealand.

Introduction

Historical moderate to large magnitude earthquakes that ruptured the ground surface provide important constraints for the geometries and displacements of the faults that accommodated these earthquakes, and are used to estimate seismic hazard in New Zealand and overseas (e.g., Smith and Berryman, 1986; Wells and Coppersmith, 1994; Stirling et al., 1998, 2002, 2012; Wesnousky, 2008; McCalpin, 2009; Biasi et al., 2013; Field et al., 2014, 2015; Hecker et al., 2013; Schwartz, 2018; Page 2020). These rupture data permit calculation of the magnitudes of prehistoric earthquakes from paleoseismic observations where there are no instrumental measurements or records of the damage arising from the event (Stirling et al., 2012; 2013). More recently, information on the dimensions and displacement of surface-rupturing historical earthquakes has been used to estimate the likelihood of rupture termination at fault irregularities (e.g., steps and bends) or the maximum distances that earthquakes can jump between individual faults (Wesnousky, 2008; Biasi and Wesnousky, 2016).

Historical surface-rupturing earthquakes in New Zealand demonstrate the importance of complex multiple-fault rupture (Beanland et al., 1989; Hull, 1990; Beavan et al., 2012; Grapes and Holgate, 2014; Litchfield et al., 2018; Nicol et al., 2018; Humphrey and Nicol, 2020; Table 1, Figs 1 & 3, Appendix 1 Figs A1-A8). Multiple-fault ruptures (here after referred to as multi-fault) during earthquakes have also been recorded globally in a range of tectonic setting and locations. These earthquakes include; the 1958 Gobi Altay Earthquake (Kurushin et al., 1997), 1992 M_w 7.3 Landers (e.g., Sieh et al., 1993), 1999 M_w7.9 Chi Chi (e.g., Yue et al., 2005), 2010 Mw 8.2 Denali Earthquake (Schwartz et al., 2012), 2010 M_w 7.2 El-Mayor Cucupah (e.g., Fletcher et al., 2014), 2012 Mw 8.2 offshore Sumatra (e,g., Satriano et al., 2012), and the 2018 M_w 6.1 Hualien earthquakes (e.g., Lajoie et al., 2019).

In this report we primarily use analysis of historical New Zealand surface-rupturing earthquakes to examine the following questions.

1. What were the geometries and displacements of surface rupture during New Zealand historical earthquakes?
2. How common are ruptures of multi-faults for New Zealand earthquakes?
3. What factors influence the geometry and number of constituent faults in multi-fault ruptures and whether the geometric rules that constrain the occurrence of multi-fault ruptures in California (e.g., Biasi and Wesnousky, 2016) also apply to New Zealand?
4. Do different rupture scenarios (e.g., fault segmentation and multi-fault rupture) significantly impact the frequencies and magnitudes of large events, and the resulting seismic hazards?

To address these questions we combine data from the literature with analysis of lidar datasets to remap surface-rupture geometries and displacement for eight New Zealand historical earthquakes (Fig. 1, Table 1 and Appendix 1). These maps have been used to quantify the variability of surface-rupture geometries and displacement, and to consider how best to capture the full range of fault-rupture geometries in future National Seismic Hazard Models (NSHM) for New Zealand. The spatial distributions of co-rupturing faults (e.g., spacings and intersection relationships) have been described to quantify the length-scales over which synchronous rupture of multiple faults occurred. Measurements of rupture length and single-event average displacement (hereafter referred to as average displacement) for individual faults in historical earthquakes have been compared to estimates of these parameters for the same faults using existing empirical relations for earthquakes on 'single' faults. These comparisons permit the examination of how the displacements and rupture length for individual faults varies depending on whether a fault ruptures in isolation from other

faults (i.e., single-fault rupture) or together with other faults (i.e. multiple fault rupture) during large-magnitude surface-rupturing earthquakes. The available data indicate that the rupture of multiple faults during individual earthquakes has been common in New Zealand during the last ~180 years. These multi-fault ruptures occur for a range of fault types and earthquake magnitudes, and in different tectonic settings. All multi-fault ruptures are part of interconnected fault networks. Multi-fault ruptures were included for some major faults in the 2010 NSHM (Stirling et al., 2012), and are more numerous in the 2022 New Zealand NSHM. Inclusion of multi-fault earthquakes in the NSHM is expected to increase the magnitudes and decrease the frequency of >Mw 7 earthquakes.
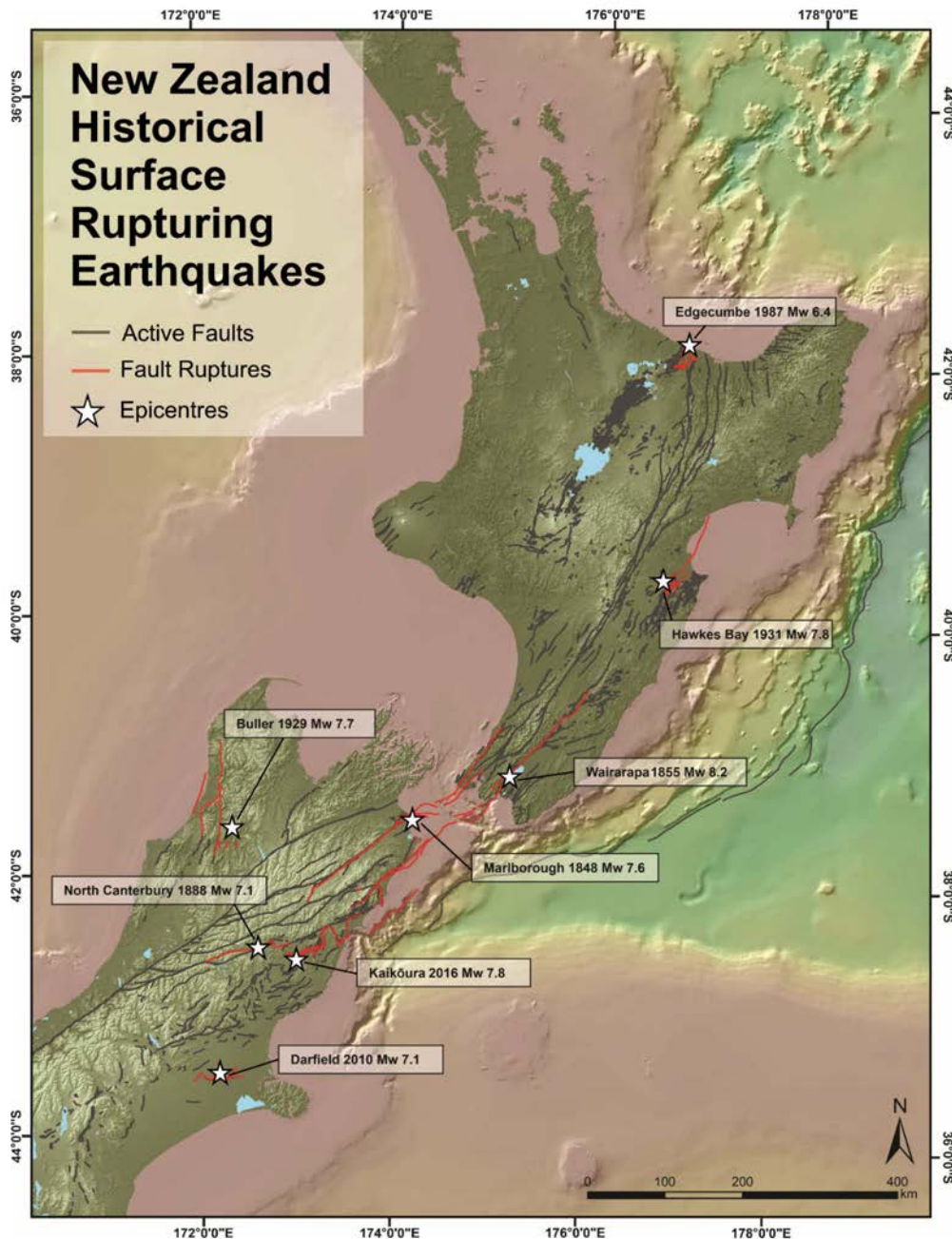

Figure 1. *Map showing the locations of the eight historical surface-rupturing earthquakes studied in this report. Red lines and epicentre locations are from the maps in the appendices. Mapped and inferred surface ruptures from these earthquakes are indicated by the red lines. Grey lines show GNS active faults (Langridge et al., 2016). Hikurangi plate interface from QMAP (Edbrooke et al., 2015). (https://data.gns.cri.nz/rgmad/datadict/GMNZ1M/2014/NZL_GNS_1M_geology.html). Refer to Table 1 for details of each earthquake and Appendix 1 Figures A1-A8 for fault-rupture maps.*

Data and methods

To understand better the geometries of earthquake ruptures and the importance of multi-fault ruptures for earthquake magnitudes, recurrence intervals and average displacement we utilise information for eight surface-rupturing historical earthquakes in New Zealand since historical written records began in 1840. Details of these earthquakes are presented in Table 1, while the locations of the surface rupturing faults and their temporal distributions are shown in Figure 1. The magnitude-time relationships for these earthquakes are shown for multi-fault and single-fault (red and green filled circles) earthquakes in Figure 2, with broad clustering of earthquake activity in New Zealand into three main time periods, ~1840-1865, ~1920-1942 and ~2010-2022.
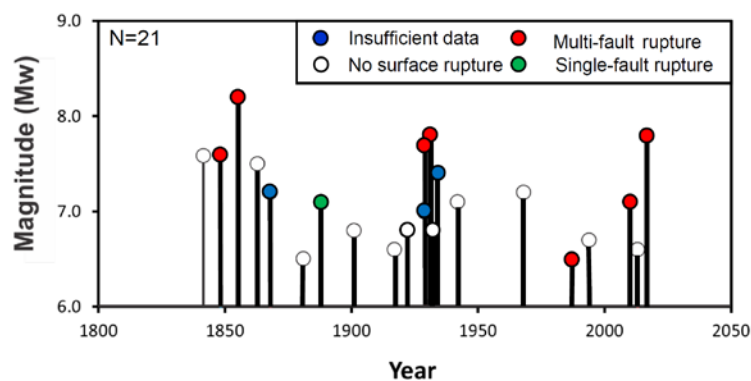

Figure 2. Stick plot showing the temporal distribution of earthquakes of Mw ≥6.4. Surface-rupturing earthquakes interpreted in the literature to have produced displacement on multiple faults are indicated by the red filled circles. Fault geometries for earthquakes that did not rupture the ground surface (white filled circles) are unknown. The multi-fault and single fault surfaces (red and green circles) are studied here, while the three earthquakes marked by blue filled circles (1868 Mw 7.2 Cape Farewell, 1929 Mw 7.1 Arthurs Pass and 1934 Mw 7.4 Horoeka) are believed to have ruptured the ground surface, but are constrained by insufficient data to be included in this study. For further details of the historical earthquakes refer to Table 1, Downes and Dowrick (2014) and Nicol et al. (2016a).

For each of the eight earthquakes listed in Table 1 we have remapped the surface traces of rupture and estimated average displacement using a combination of historical accounts and rupture maps, previous publications, reanalysis of the isoseismal maps from Downes and Dowrick (2014), and remapping of the ruptures using post-earthquake lidar and paleoseismic studies (e.g., Beanland et al., 1989; Hull, 1990; Kelsey et al., 1998; Litchfield et al., 2006; Mason and Little, 2006; Rodgers and Little, 2006; Khajavi et al., 2016, 2018; Humphrey and Nicol, 2020; Manighetti et al., 2020). The quality of the fault-rupture maps available from historical accounts generally decreases with time, with pre-1930 data often less complete than post-1930 maps (see maps in Appendix 1). The best datasets available are from the 2010 Darfield and 2016 Kaikōura earthquakes, which have been studied using extensive remote (e.g., lidar, InSAR and aerial photography) and GPS datasets that constrain both faulting of the ground surface and displacement on faults at depth (e.g., Beavan et al., 2012; Zinke et al., 2019; Howell et al., 2020). The resulting fault-rupture geometries, lengths and average displacement for historical New Zealand earthquakes are compared with a compilation of international surface-rupturing earthquakes from Wesnousky (2008) to assess whether established international models for rupture lengths and displacement also apply to New Zealand. Lastly, we

compare historical rupture-dimensions and slip magnitudes with geological estimates of these parameters to consider if the new data and analysis could provide input to future fault-rupture models that underpin the New Zealand NSHM.

For the 1931 Hawkes Bay and 1987 Edgecumbe earthquakes lidar-derived DEMs produced in the last 15 years were used in conjunction with historical accounts of surface ruptures to remap fault traces and displacement. The lidar-derived DEMs have a ~10-20 cm vertical resolution and comparable to fault-rupture maps generated from field mapping immediately after each earthquake (Henderson 1933; Beanland et al., 1989). In addition to constraining rupture of the ground surface, the lidar permitted identification of monoclinal warps of the ground surface (heights <0.5 m and ~10s m wavelength). These monoclonal warps typically form along the tips of the scarps and can be difficult to identify in aerial photographs or from ground-based mapping of fault rupture (Hull, 1990; Beanland et al., 1989; Begg and Mouslopoulou, 2010). Along-fault displacement profiles of warps and scarps were constructed to determine where discrete surface ruptures and monoclinal flexures accommodate similar throws on the same fault; where the throws were comparable they were assumed to have accumulated at least partly in the historical earthquake. Use of the lidar yielded fault traces that were typically <20% longer than the traces mapped immediately following the earthquake.

Table 1. *Summary of the eight New Zealand historical (1840-2022) surface-rupturing earthquakes that form the focus of this study.*

Name	Fault[¥]	Year	Magnitude (Mw)	Dominant Slip Type[§]	Average Displacement[†] (m)	Rupture Length[¥] (km)	Number faults ruptured	References
Marlborough	Awatere	1848	7.6	S-Slip	5.3±1.6	105±5	1-3	Mason and Little (2006) Little et al. (2009), Grapes and Holgate (2014)
Wairarapa	Wairarapa	1855	8.2	S-Slip*	7.35±1	102±8	≥3	Rodgers and Little (2006), Grapes and Holgate (2014), Manighetti et al. 2020
North Canterbury	Hope	1888	7.1	S-Slip	1.6±0.3	60±20	1	Cowan (1990), Khajavi et al. (2016 & 2018)
Buller	White Creek	1929	7.7	R[‡]	4.5±0.5	110±10	≥3	Henderson (1937), Berryman (1980), Downes and Dowrick (2014), Hancock et al. (2015), Humphrey and Nicol (2020)
Hawke's Bay	Napier	1931	7.8	R	4.6±0.5	75±10	≥3	Henderson (1933), Hull (1990), Downes and Dowrick (2014
Edgecumbe	Edgecumbe	1987	6.4	N	1.05±0.35	15.5±2	≥7	Beanland et al. (1989)
Darfield	Greendale	2010	7.1	S-Slip	2.5±0.1	29.5±0.5	≥5	Beavan et al. (2012), Quigley et al. (2012)
Kaikōura	Jordan-Kekerengu-Needles	2016	7.8	S-Slip, R	5.5±1	88±10	≥17	Litchfield et al.(2018), Zinke et al. (2019), Howell et al. (2020)

[¥]Primary fault. [§]Slip Type: S-Slip, strike slip; R, reverse; N, normal. *Minor reverse. [‡]Minor strike slip. [†]Average displacement at the ground surface on the primary fault during the earthquake.

Surface ruptures and displacement for the Darfield and Kaikōura earthquakes were mapped using a combination of field mapping and interpretation of lidar DEM hillshade models. For the purposes of this study we have mainly adopted the surface rupture maps produced immediately following the earthquakes and published in the literature (Quigley et al., 2012; Litchfield et al., 2018). We have augmented and modified the original fault maps for the Kaikōura Earthquake using optical satellite imagery and aerial photographs to measure displacements of the ground surface (Zinke et al., 2019; Howell et al., 2020). Field mapping of the Darfield and Kaikōura earthquake surface ruptures were also augmented by GPS modelling of ground deformation and coastal measurements of uplift, which were used to map subsurface faults that ruptured during these earthquakes (Beavan et al., 2012; Clark et al., 2017; Mouslopoulou et al., 2019; Nicol et al., 2022). GPS data similar to that collected for the Darfield event are not available for earthquakes prior to 2010, however, geodetic relevelling surveys provide useful information for the Hawkes Bay 1931 and Edgecumbe 1987 earthquakes (Darby, 1987; Blick and Flaherty, 1989). Relevelling surveys in the region of the 1987 Edgecumbe Earthquake ground rupture suggest that this earthquake could have ruptured the Matata Fault at depth (Fig. 3), producing a 50-100 m wavelength warp at the ground surface with vertical separation of ~0.5 m.

Given the large dataset available to constrain fault displacement and rupture geometries, the post-2000 earthquakes are likely to be characterised by the highest resolution data, with the potential for incomplete rupture maps increasing as the date of the historical rupture increases from the present. The locations, geometries and displacement of surface fault ruptures and sub-surface fault slip during the 1848, 1855, 1888 and 1929 earthquakes are poorly constrained compared to the 1987, 2010 and 2016 earthquakes. Surface ruptures during these pre-1930 earthquakes are primarily characterised by historical accounts of the earthquakes and by subsequent geological investigations (Henderson, 1937; Berryman, 1980; Cowan, 1990; Downes, 1995; Grapes et al., 1998; Mason et al., 2006; Rodgers and Little, 2006; Litchfield et al., 2010; Khajavi et al., 2018; Grapes and Holgate, 2014; Humphrey and Nicol, 2020). In addition to on-fault observations, the locations and geometries of surface ruptures during pre-1930 earthquakes was defined by the spatial distributions of landslides (Downes and Dowrick, 2014; Hancox et al., 2015). Despite the wealth of available data, uncertainties remain about the number and length of faults that ruptured in pre-1930 earthquakes. These uncertainties arise for a number of reasons including; the remoteness of the earthquakes at the time of rupture (e.g., 1848 & 1888 earthquakes), the presence of thick native forest cover (1929 earthquake), the difficulty of unambiguously interpreting whether reported 'fissuring', land 'uplift' or 'subsidence' reflect fault rupture or alternate processes, such as landsliding (e.g., 1848, 1855, 1888 & 1929 earthquakes), rupture passing offshore (1848, 1855, 1929 and 1931 earthquake), and doubt surrounding whether ground rupture was partly due to large aftershocks rather than the main event (e.g., 1848, 1855 and 1929 earthquakes). For these reasons, much of our analysis is focused on the 1987, 2010 and 2016 earthquakes.

For the maps presented in Appendix 1 we show rupture traces mapped as probable (solid red lines) or possible (red dashed lines), depending on our confidence in assigning surface rupture to each fault. In particular, lower confidence surface rupture traces for the 1848 and 1855 earthquakes are primarily from Grapes and Holgate (2014), for 1929 from Humphrey and Nicol (2020) and for 1931 from this study. For the eight earthquakes studied, we have not attempted to map sub-surface slip on the Hikurangi Plate interface, although it has been inferred to have accompanied rupture of upper-plate faults in 1855, 1931 and 2016 (Walcott, 1978; Ishibashi, 1987; Darby and Beanland, 1992; Beavan and Darby, 2005; Rodgers and Little, 2006; Bai et al., 2017; Mouslopoulou et al. 2019). The presence of shallow dipping reverse faults that do not intersect the ground surface onshore,

and are therefore difficult to sample, represent a major point of difference between New Zealand and other steeply dipping (mainly strike slip) fault systems, where many of the key faults encountered at the surface can be assumed to be representative of the entire crust (e.g., California).

We have estimated the number of individual faults that ruptured in each earthquake together with their fault rupture lengths, average displacement and magnitudes. In addition, we have estimated the total rupture length and average fault displacement for all individual ruptures in each of the eight earthquakes outlined in Table 1. Measurement of fault lengths and displacement for individual faults required subjective decisions to be made about what constitutes a single fault. Here we use a combination of criteria to identify individual faults at a regional scale (≥1 km long and ≥0.1 m average displacement) including, fault strike and dip direction, two-dimensional physical separation of traces (in map view) and fault-slip type. For the most part, our individual faults correspond to faults that had previously been assigned different names and were considered to be geometrical distinct structures. A notable exception is the Needles-Kekerengu-Jordan-Upper Kowhai faults that ruptured in the 2016 Kaikōura Earthquake and, in this study, are considered to be a single structure due to their similarity in strike and dip direction, and predominance of right-lateral displacements (Kearse et al., 2018; Howell et al., 2020). Rupture lengths for individual faults were measured from the fault-trace maps in Appendix 1 and from less direct measures including, uplift, landslides and isoseismals. Uncertainties on these lengths and associated error bars in each of the graphs reflect the range of possible lengths using both high confidence (probable) and low confidence (possible) rupture traces. In addition to rupture lengths, we have measured 'Geological Fault Lengths' from the 1:250000 QMAP geological maps and the published literature (e.g., Rattenbury et al., 1998, 2006; Begg and Johnston, 2000; Lee and Begg, 2002; Nathan et al., 2002; Mouslopoulou et al., 2008; Leonard et al., 2010; Lee et al., 2011). Average earthquake displacement have mainly been derived from the published literature (e.g., Berryman, 1980; Beanland et al., 1989; Hull, 1990; Mason and Little, 2006; Quigley et al., 2012; Khajavi et al., 2016, 2018; Litchfield et al., 2018; Manighetti et al., 2020). Where possible, we have integrated the displacement for along-strike profiles to estimate the average displacement on individual faults. For example, we used the 1855 slip profile along the Wairarapa Fault from Manighetti et al. (2020) to estimate average slip of 7.35±1 m, which is ~40% of the ~18 m maximum slip from Rodgers and Little (2006). In cases where it was possible for displacement profiles to be generated for historical ruptures the average displacement is typically 40-50% of the maximum. In the case of the 1929 Buller Earthquake few displacement data are presently available for the White Creek Fault and we have adopted the 4.5±0.5 m vertical displacement of state highway 6 (Henderson, 1937), as the average slip (although this value could be in error by a factor of two).
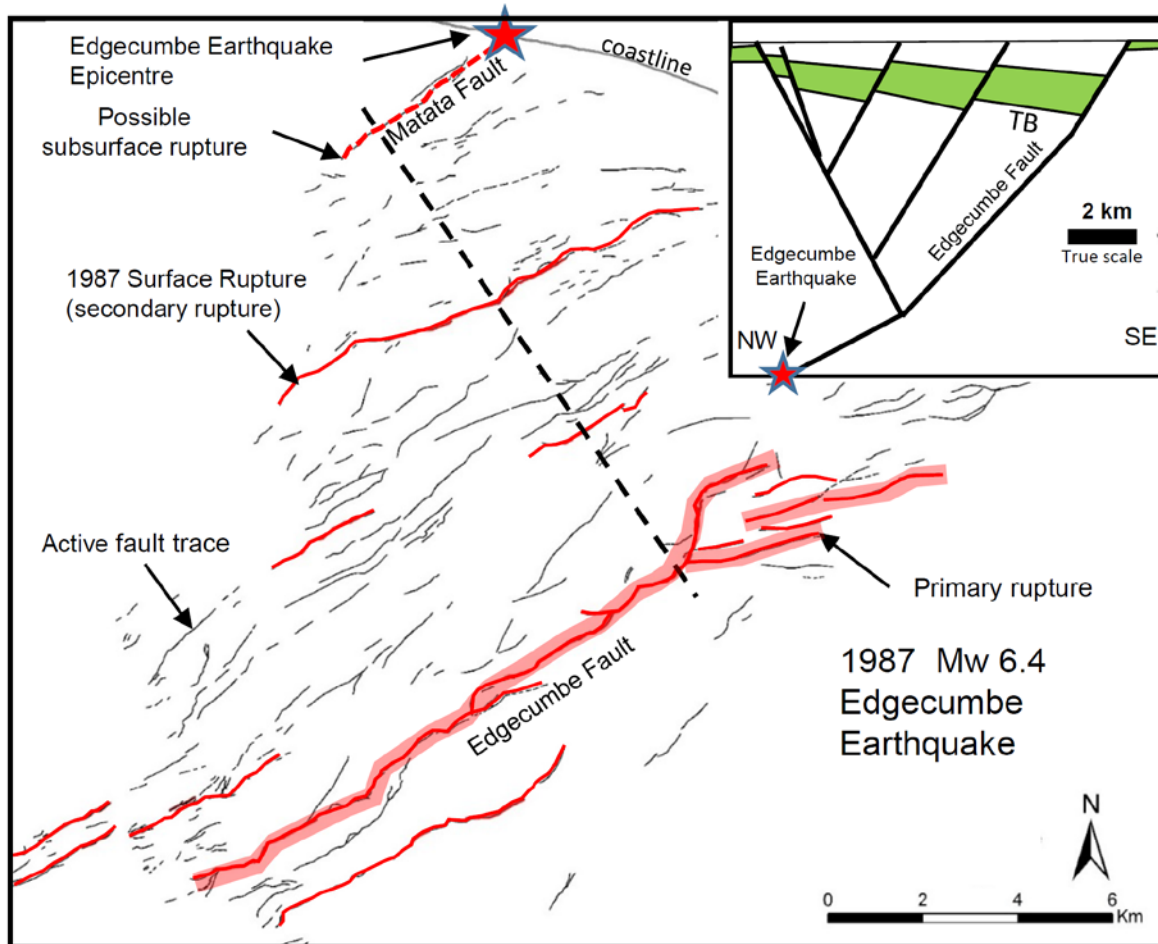
Figure 3. Map and simplified cross section (inset) showing fault surface rupture during the 1987 Mw 6.4 Edgecumbe Earthquake. Surface ruptures were mapped using a combination of fieldwork from Beanland et al (1989), lidar mapping (this study) and interpretation of 1950s vintage aerial orthophotographs (this study). Thin red lines show interpreted surface ruptures from 1987. The Edgecumbe Fault is the longest surface trace and is defined as the primary fault, and shown by the red polygonal along the fault trace. Thin black lines are mapped active fault traces that do not appear to have ruptured in 1987. The red star shows the earthquake epicentre location from Downes and Dowrick (2014). Dashed black line on the map shows the location of the cross section. TB in the cross section indicates the top of the Torlesse Supergroup basement rocks from Mouslopoulou et al. (2008).

Fault rupture geometries and kinematics

Of the eight earthquakes studied here all except the 1888 North Canterbury event display evidence for more than one fault rupturing the ground surface (Beanland et al., 1989; Hull, 1990; Beavan et al., 2012; Grapes and Holgate, 2014; Humphrey and Nicol, 2020)(Figs 1 & 3, Table 1 and Appendix 1 Figs A1-A8). The complexity of these ruptures and the number of faults they co-rupture are variable, with the Mw 7.8 2016 Kaikōura apparently being the most complex earthquake (cf. Litchfield et al., 2018), where complexity is here defined by the number of faults that ruptured and the variability in their orientations. It is worth noting, however, that the apparent complexity of multi-fault ruptures is likely to be strongly dependent on the resolution of the earth-deformation measurements, which is impacted by the date and magnitude of the earthquake. As a general rule the number and complexity of faults that ruptured during each earthquake increases towards the present day (again possibly due to an increase in data resolution with time). For example, prior to 1932 the minimum number of faults that ruptured during each earthquake ranged from 1-3, while after 1980 it ranged from 5-17. Moderate magnitude earthquakes (e.g., Mw 6-6.5) with smaller average displacements

could also rupture multiple faults with similar complexity to larger earthquakes, although much of this complexity may be sub-resolution (i.e., it remains possible that the complexity is independent of fault size).

Given these completeness issues with increasing time before present, it is difficult to determine precisely how many faults (on average) ruptured in each earthquake. A minimum estimate can be inferred from the historical data as a total of at least 41 faults ruptured in eight separate earthquakes since 1840, with each earthquake rupturing an average of about five faults. If we assume that the Kaikōura Earthquake was an event of unusual complexity and exclude it from our calculation, 24 faults ruptured in seven earthquakes, the minimum average number of faults ruptured per earthquake of about 3.5. These minimum values are likely to increase in the future as the resolution of earthquake-deformation data continues to improve. As an illustration of this point, the minimum average number of faults that ruptured in the 1987, 2010 and 2016 earthquakes is about 10.

The fault geometries and kinematics of surface fault ruptures show both differences and similarities between earthquakes. Where 1931 and older earthquakes rupture more than one fault, these faults are mainly characterised by sub-parallel traces that are connected along strike. For example, the Wairarapa, Alfredton and Wharekauhau faults ruptured together during the 1855 Wairarapa Earthquake (Appendix Fig. A2). In the Awatere 1848 and Hawkes Bay 1931 earthquakes it is also possible that multiple fault ruptures are separated by up to 10 km across the strike of the fault system (Appendix Figs A1 & A5). In the 1931 Hawkes Bay earthquake the southern Napier and Poukawa faults ruptured together and are separated by ~8 km across strike, and were connected during the earthquake by a strike-slip fault (Hull, 1990). Similarly, the Ohariu and Wellington faults may have ruptured during the 1848 Awatere earthquake, and in this case linkage of the two faults is inferred to occur offshore in Cook Strait (Grapes and Holgate, 2014).

Given the paucity of data for the 1931 and older earthquakes, we believe that their surface ruptures were probably more complex than has been presented in the literature or recorded by the maps in the Appendix 1. To emphasise this point, in the 2010 Darfield Earthquake only the Greendale Fault ruptured the ground surface and if this earthquake had occurred prior to 1932 (i.e., prior to deployment of GPS stations or dense seismograph networks), it would likely have been characterised as an earthquake that ruptured a single fault.

The geometries of fault ruptures during the 1987 Edgecumbe (Fig. 3), 2010 Darfield and 2016 Kaikōura earthquakes are generally more complex and comprise of more constituent faults (i.e. ≥7, ≥5 and ≥17 faults ruptured in the 1987, 2010 and 2016 earthquakes, respectively), than those formed pre 1987 (Appendix 1 Figs A1-A8). The 1987 Edgecumbe Earthquake ruptured normal faults across most, or all, of the ~15 km width of the Taupo Rift (Figs 3 & A6). The Edgecumbe Fault was the primary fault that ruptured the ground surface during the earthquake and is accompanied by at least an additional six fault traces. In addition, the Matata Fault may have ruptured at depth in 1987 (i.e., the Matata Fault did not rupture the ground surface). All faults that ruptured the surface in 1987 strike sub-parallel to each other at ~050° and, with the exception of splays at the northern tip of the Edgecumbe Fault, do not intersect in map view. However, the Edgecumbe or Matata faults bound the rift system in the region of the earthquake and in cross section most faults that ruptured in 1987 are here interpreted to intersect either the Edgecumbe or Matata faults at depth (Fig. 3 inset cross section).

The Darfield and Kaikōura earthquakes differ from the Edgecumbe ruptures as in both cases their constituent faults vary in strike by up to ~90° and display a range of slip types. In the Darfield Earthquake the Greendale Fault mainly strikes approximately east-west and was primarily right-

lateral, while the more northerly striking Hororata, Charing Cross, Charing Cross North and Sandy Knolls faults accommodate a significant component of reverse displacement (Beavan et al., 2012; Quigley et al., 2019). All of these faults are modelled to intersect the Greendale Fault forming a central 'backbone' structure, which the secondary faults mainly terminate against. By contrast, the Kaikōura Earthquake did not comprise a single 'backbone' fault or a completely connected set of surface ruptures. Instead, the Kaikōura Earthquake surface ruptures comprise two main areas of faulting separated by the Hope Fault and up to 10 km distance (Hamling et al., 2017; Litchfield et al., 2018). Subsequent mapping and modelling suggests that these surface ruptures may be linked at depth by a thrust fault, which could be the northeastern continuation of the Hundalee Fault, and passes beneath the Hope, Papatea and Upper Kowhai-Kekerengu faults (see Nicol et al., 2022 and references therein). Therefore, a key inference from the 1987, 2010 and 2016 ruptures is that the network of faults that ruptured were all hard-linked. However, in all three cases the extent of fault linkage was not apparent from surface exposures alone and can only be inferred from the fault geometries at the surface (1987 earthquake) or from modelling of surface displacements (2010 and 2016 earthquakes). In the Kaikōura Earthquake these fault linkages directly reflect the presence of shallow-dipping faults (e.g., ≤30°) in the sub-surface and the 1987, 2010 and 2016 events highlight the importance of understanding the three-dimensional geometries of faults when developing plausible fault-rupture models for the purposes of earthquake hazard assessment.

The 1855, 1931, 2010 and 2016 earthquakes ruptured faults with variable slip sense. In cases where the individual faults in multi-fault ruptures have variable strikes, changes in fault strike often influence the relative importance of strike slip and dip slip. For example, in the 1931 earthquake the northeast striking Napier and Poukawa faults with predominately reverse slip (Hull, 1990; Kelsey et al., 1998) are connected by a strike-slip fault that strikes southeast at a high angle to the reverse faults (Appendix 1 Figure A5). Similarly, during the Kaikōura Earthquake faults striking 070-100° were predominantly right-lateral strike-slip, while faults striking between 020° and 060° accommodate a combination of reverse slip (and associated hanging-wall uplift) and strike-slip (Litchfield et al., 2018; Nicol et al., 2018). The kinematics of the faults that ruptured the ground surface in 1931, 2010 and 2016 are broadly compatible with the ~250-270° trend of the relative plate motion vector in the rupture areas, with slip vectors on nearby faults from geological data (Kelsey et al., 1998; Van Dissen and Yeats, 1991; Nicol and Wise, 1992), and with the trends of regional principal stress ($\sigma 1$) or the Principal Horizontal Shortening (PHS) direction of 100-140° determined for these regions (Nicol and Wise, 1992; Balfour et al., 2005; Sibson et al., 2011; Townend et al., 2012). The first-order conclusion from these observations is that fault slip rake is generally consistent with the regional stress and strain fields and the fault strike, which has two main implications. First, substantial changes in the regional orientations of the principal stress axes are not required to account for the first-order orientations of fault-slip rake in New Zealand historical earthquakes. Second, in the absence of slip data for active faults it should be possible to predict the first-order slip rake from the fault strike and dip, and the regional stress field orientations (e.g., Shaw et al., 2022).
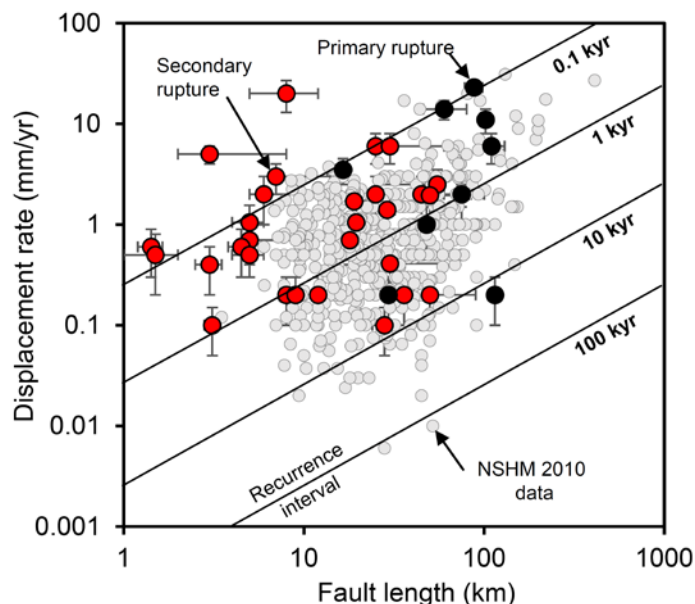
Figure 4. *Plot of slip rate vs fault-rupture length for historical surface-rupturing earthquakes (this study) and data from the 2010 NSHM model (Stirling et al., 2012). Primary faults in historical earthquakes (filled black circles) and secondary faults (filled red circles) are shown with error bars. Contours of recurrence interval (RI) are indicative only and were derived using the fault lengths (L) to estimate single-event displacements (i.e. average displacement, D_{ave}) using the equation $D_{ave}=0.03xL$ (derived for rupture lengths <120 km in Wesnousky, 2008) and the $D_{rate}= D_{ave} /RI$ equation.*

Fault lengths, average displacement and displacement rates

Fault-rupture lengths, average displacements and displacement rates (Fig. 4) are widely recorded for both historical and prehistorical earthquakes (e.g., Wells and Coppersmith, 1994; Wesnousky, 2008; Stirling et al., 2012; Hecker et al., 2013; Biasi and Wesnousky, 2016; Nicol et al., 2016b). Fault length and average displacement are important parameters for estimating rupture areas and moment magnitudes (Mw) for active faults that have not ruptured historically, while displacement-rate helps to constrain the rate of earthquakes and their recurrence intervals for seismic hazard assessment. Determining whether rupture length, average displacement and slip-rate scaling are different for earthquakes that rupture single faults and multiple faults during the same earthquake is key for understanding whether multi-fault ruptures should be treated differently than single-fault earthquakes in seismic hazard models. The difficulty in making this assessment is that average displacements and lengths measured from historical surface ruptures on single faults could, in some cases, record values for the primary fault in multi-fault ruptures. For example, the average displacement and length data for the Edgecumbe Fault are included in international compilations for individual faults (e.g., Wesnousky et al., 2008) and this fault is one of at least seven that ruptured during the Edgecumbe Earthquake (Fig.3). Therefore, while comparison of our data to the international literature may provide information about single-fault vs multi-fault ruptures, it may equally provide information of the scaling relationships between primary fault and secondary fault ruptures (with the international literature being also being dominated by multi-fault ruptures representative of primary fault ruptures).

The relationships between fault displacement rates and length for historical earthquakes in New Zealand and for the 2010 NSHM are shown in Figure 4. Displacement rates and rupture lengths for faults that experienced historical earthquakes (red and black filled circles) range from 0.1 to ~20 mm/yr and 1.5-115 km, respectively (Fig. 4). The plot in Figure 4 shows a weak positive correlation, with longer faults tending to have higher displacement rates, with the trend of the data-cloud being

14

approximately parallel to the lines of equal recurrence interval. The weak positive relationship between displacement rate and length has been widely observed in the literature, where it has been interpreted to at least partly reflect strain localisation onto the longer faults and associated increase in fault maturity (Bingham and Bodin, 1992; Wells and Coppersmith, 1994; Nicol et al., 2005, 2010). The correlation of displacement rate versus length graph are typically better than Fig. 4 where the data are derived from individual fault systems or tectonic domains (Nicol et al., 2005). Therefore, the wide spread in displacement rates for a given fault length can be attributed to the data being sourced from different tectonic domains with a range of regional strain rates. For example, fault and earthquakes from the high strain 'core' of the plate boundary are expected to be focused in the upper half of the present data cloud. The displacement rate vs length plot shows almost complete overlap between the historical earthquake and 2010 NSHM datasets (Stirling et al., 2012)(Fig. 4), which supports the use of the NSHM data for seismic hazard assessment. The broad similarity of the two datasets also suggests that the displacement-rate and length relationships are not noticeably different for the individual faults depicted in the 2010 model and for the faults that ruptured historically, mainly as part of multi-fault ruptures.
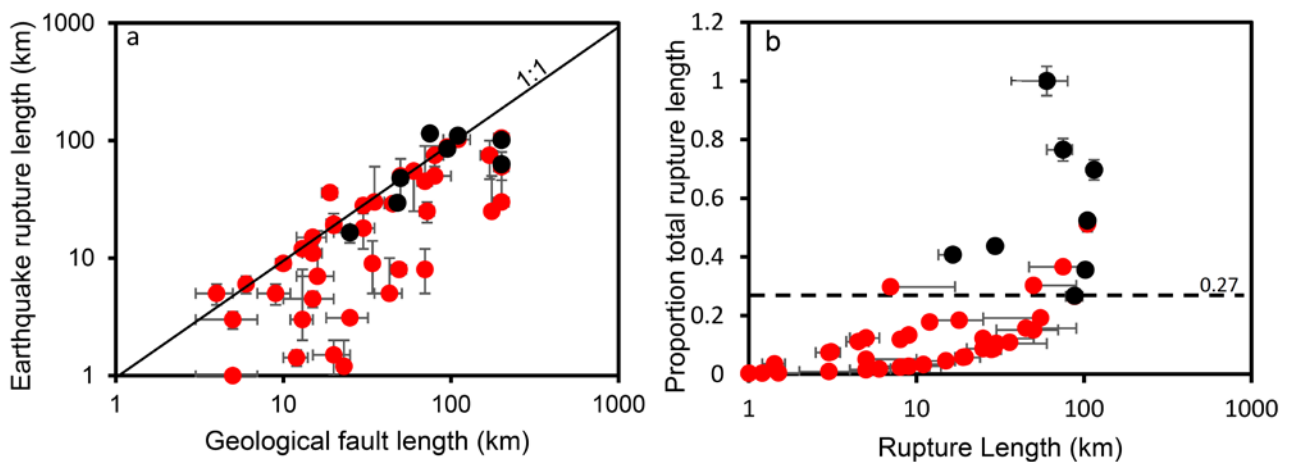

Figure 5. Fault-lengths for New Zealand historical surface-rupturing earthquakes. a) Relationship between earthquake rupture length and geological fault length (see text for definitions). 1:1 line is shown for reference. b) Fault-rupture length for individual faults plotted against their length as a proportion of the total measured rupture length for each earthquake. The 0.27 horizontal dashed line marks the minimum proportion of total rupture length for a primary fault. Individual primary (black filled circles) and secondary faults (red filled circles) are differentiated on the graphs.

Fault earthquake rupture length and geological fault length have been measured for individual faults in historical New Zealand earthquakes (Fig. 5a). The available data generally plot on, or beneath, the 1:1 line suggesting that geological fault lengths are typically (although not exclusively) longer than, or equal to, earthquake rupture lengths for both primary and secondary faults. The data indicate earthquakes rupture varying amounts of the total fault length in bedrock. On average, rupture length is ~0.8 (~80%) of geological fault length for primary faults and ~0.6 (~60%) of geological fault length for secondary faults. In detail, Figure 5a shows that historical earthquakes may rupture 0.05-1.9 of the total geological fault length for secondary faults and 0.3-1 for primary ruptures. Numbers >1 arise because the entire rupture lengths were not previously mapped in bedrock (e.g., The Humps Fault, 2016 Kaikōura Earthquake), while part-ruptures (<1) could indicate that only a portion of the geological fault is active or, more likely, that about two-thirds of the faults sampled only rupture sections of active faults. Long strike-slip faults (Hope and Awatere faults) are the most notable

examples of partial ruptures and indicate that these faults often rupture in segments or sections, as has been proposed in the literature (e.g., Mason and Little, 2006; Little et al., 2009; Grapes and Holgate, 2014; Khajavi et al., 2016, 2018). Therefore, the available data support a mixed mode rupture model where earthquakes rupture all or part of (typically >30% of their geological lengths) individual faults that collectively produce multiple fault earthquakes. Such a model could be considered a mix of segmentation and multi-fault rupture models. However, unlike the classical fault segmentation 'Characteristic Model' (Schwartz and Coppersmith, 1984), where each fault segment ruptures in its entirety with characteristic maximum or average displacement, successive earthquakes on the same fault may rupture different parts of the fault and could be accompanied by rupture on different nearby faults. Thus, the concept of a characteristic earthquake may not apply to these multi-fault events, even if their average (or maximum) displacements are similar in successive earthquakes (see 'Controlling factors' and 'Frequency' sections for further discussion).

As more detailed surface and sub-surface deformation data becomes available for individual earthquakes it is likely that we will discover that, on length-scales of a kilometre or more, most earthquakes rupture multiple faults. In such cases, it will be important to estimate how much the earthquake was focused on the primary structure and how close these multi-fault earthquakes are to single-fault events. In extreme cases, it may be that so little of the stress, displacement or seismic moment was focused on secondary faults that, for seismic-hazard purposes, they could be considered a single-fault rupture. We find that individual primary faults constitute between 0.3 and 1 (30-100%) of the total rupture length, while individual secondary faults typically account for <0.2 (20%) of the total rupture length (Fig. 5b). However, while individually secondary faults may constitute only a small proportion of the total rupture length (<20%), collectively they may accommodate up to 70% of the total rupture length. These proportions highlight the important contribution that secondary faults could make to the total rupture area, although they are likely to account for a smaller proportion of the total seismic moment (compared to total length).

An important question for seismic hazard is whether individual faults that form components of multi-fault ruptures have average displacements similar to what we would expect if each fault ruptured in isolation. In Figure 6a we explore the displacement-length scaling relations for primary and secondary faults in historical New Zealand earthquakes. These data show a strong positive correlation with no significant difference between the average displacement and length scaling relations for primary and secondary faults (i.e., the best-fit lines for primary and secondary faults are comparable). By definition, primary faults are longer than secondary fault rupture lengths and it could be argued that some of this difference in length occurs because primary faults ruptured a greater proportion of the geological fault length than secondary ruptures. However, in ~70% of cases the proportion of the geological fault length that ruptured is similar for primary and secondary faults. In such cases, secondary faults are generally shorter because their underlying geological fault is shorter (see next paragraph for discussion of circumstances where this is not the case). Similarly, the observed vs calculated average displacements show comparable relationships for primary and secondary faults (Fig. 6c). The calculated average displacements were derived from global scaling relations of Wesnousky (2008) and show a similar strong positive correlation for both primary and secondary faults, which are generally exceeded by observed values. Therefore, the available displacement and length data generally do not show that average displacements differ for earthquakes that rupture one fault or multiple faults. These data appear to suggest that average displacement on individual faults is often controlled by their lengths and not by whether the faults are primary or secondary ruptures, by the size of the earthquake or by the total number of faults that it ruptures. From a seismic hazard perspective this means that in cases where fault length provides a reasonable proxy of fault size, published displacement-length scaling relations may

provide useful estimates of average (or maximum) displacement on individual faults in multi-fault ruptures. Faults that intersect or sole-out on subduction thrusts may prove exceptions to this conclusion as these low-dipping structures may significantly increase the rupture area,

Despite the relatively high R value in Figure 6a and the general accordance of the displacement-length scaling relations for primary and secondary faults (Figs 5a & 6c), two main types of outliers are observed for secondary faults in the New Zealand earthquakes, each accounting for ≤10% of the data. First, some secondary faults display low displacements for their lengths compared to all New Zealand data and could be considered 'under displaced' (Fig. 6a). These faults are interpreted to have accommodated minor triggered slip (0.1-0.3 m) during a particular earthquake. They include the Rotoitipakau Fault (~0.15 m) in the 1987 Edgecumbe Earthquake and the Hope Fault in the 2016 Kaikōura Earthquake (~0.3 m). Geological studies indicate that primary rupture of the Hope Fault could produce average displacement of ~2-4 m (Manighetti et al., 2015; Khajavi et al., 2018), which is about an order of magnitude greater than the displacement observed in 2016 (Litchfield et al., 2018). We would expect these 'under displaced' faults to be under-represented in our database as, in many cases, they are likely to be sub-resolution and may only be observed in high-resolution datasets, as illustrated by the recent discovery of two low-displacement (<0.5 m) faults that accumulated displacement during the 2016 earthquake in the Kaikōura Peninsula area (Nicol et al., 2022). A second type of outlier is observed where faults accommodate high average displacement for their recorded slip lengths. In some cases these appear to be relatively short 'linking' faults that transfer displacement between high displacement faults which are relatively long compared to the linking fault. The best example of such a linking fault is the Papatea Fault, which has a length of ~19 km and an average displacement of ~6 m, and seems to link the Needles/Kekerengu/Upper Kowhai fault and Offshore Splay Thrust Fault (Nicol et al., 2022).

We have compared the average displacement and rupture length relationships for the New Zealand earthquake data and a global compilation from historical earthquakes (Fig. 6a & 6c). This comparison suggests that for a given length average displacements for individual faults in multi-fault ruptures are generally higher than average displacements observed or calculated from the global dataset (Fig. 6a). Similarly, Figure 6c shows a strong correlation between observed average displacement for New Zealand earthquakes and calculated average displacement using rupture length a linear relation between average displacements and length from Wesnousky (2008)(see Figure 6 caption for further details). For a given length the observed New Zealand average displacements are generally higher than displacements calculated using international scaling relations (by up to a factor of 3).

Higher than average displacements for a given fault length in New Zealand (compared to average displacements from the international literature) has been previously observed and could be attributed to the rupture surface being width or length limited (e.g., Villamor et al., 2007). Length limiting due to fault intersections has the potential to produce a network of short and interconnected faults, with each fault appearing to be 'over displaced'. These faults may rupture together in multi-fault earthquakes or individually with rupture propagation terminating at fault junctions. In such networks, displacements (and stress) can be transferred between faults and while it might be possible to differentiate (and name) faults on geometric grounds they should be considered part of a single dynamic structure (i.e., the fault network). Therefore, the differences between New Zealand and global data may partly reflect the density and connectivity of the fault network and the criteria used to define individual faults.
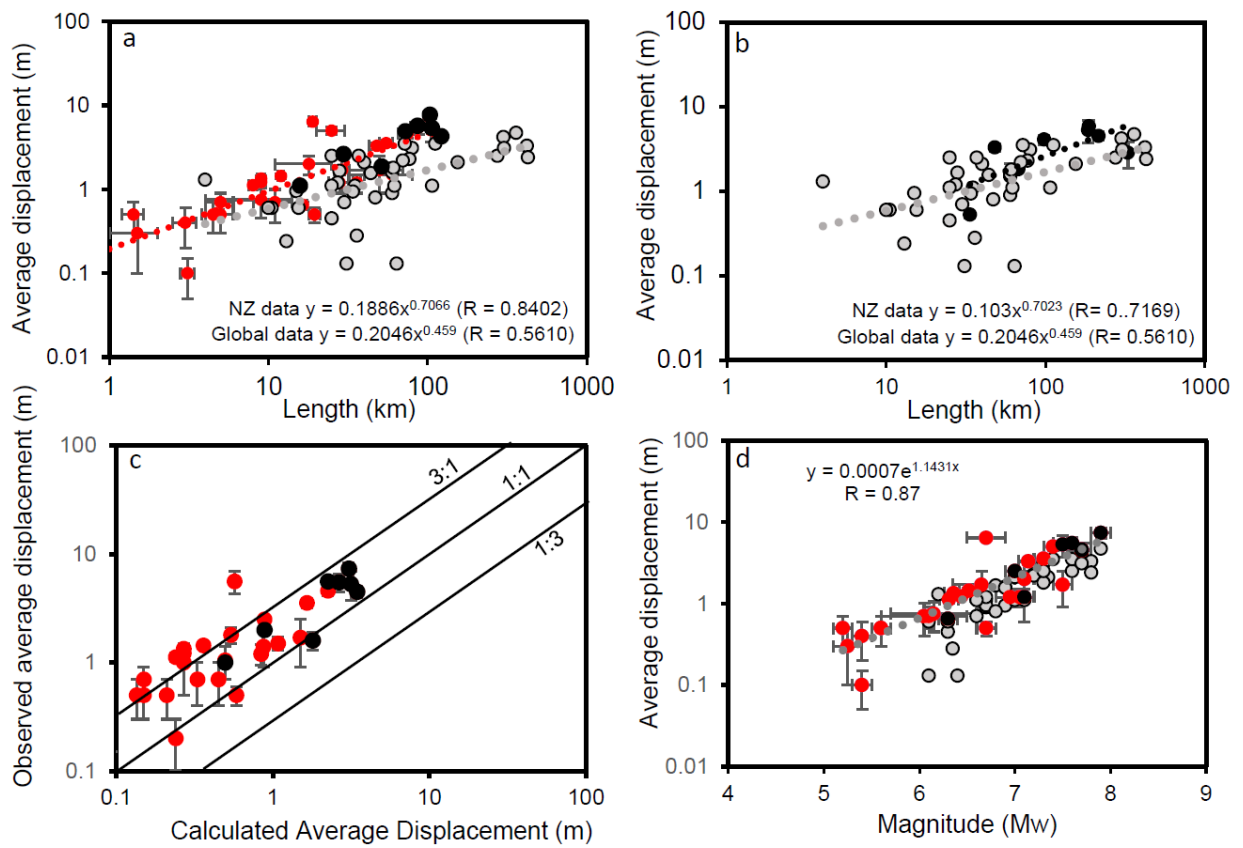
Figure 6. *Relationships between average displacement, rupture length and moment magnitude (Mw). Primary (black filled circles) and secondary (red filled circles) faults are shown, while filled grey circles indicate data from Wesnousky (2008). a) Average displacement vs rupture length plotted for individual faults that ruptured in historical New Zealand earthquakes. b) Average displacement vs rupture length plotted for all faults that ruptured in each historical New Zealand earthquake and global data from Wesnousky (2008). Average displacement in New Zealand earthquakes calculated using average displacement for individual faults weighted by their fault lengths. Lengths are the sum of fault-rupture trace-lengths for each earthquake. c) Plot comparing average displacement for individual faults that ruptured in New Zealand multi-fault earthquakes with average displacement calculated using fault lengths and a linear relation between average displacement (D_{ave}) and length (L) ($D_{ave}=0.03xL$) defined using data from Wesnousky (2008) for fault lengths of <120 km. 3:1, 1:1 and 1:3 lines are shown for reference. d) Average displacements plotted against Mw for individual primary (black) and secondary (red) ruptures in New Zealand earthquakes. Mw values are from the literature where they are typically calculated from the fault area using length and an assumed rupture depth of ~12 km (e.g., Beavan et al., 2012; Stirling et al., 2012; Litchfield et al., 2018). Mw in Stirling et al. (2012) was derived using the Mw = 4.18 + 2/3 log W + 4/3 log L (Stirling et al. 2008) and assumed Width (W) values of 10-15 km. Sensitivity testing suggests that increasing W values to 25 km to take account of increasing seismogenic thickness or decreasing fault dip does not significantly change the first-order results. In all graphs average displacement was measured or calculated for faults at the ground surface.*

As a 'test' for the multi-fault argument for the difference between New Zealand and international data we have plotted the average displacement (averaged for all measured faults) and the total length for all faults in each New Zealand multi-fault earthquake (Fig. 6b). The combined average displacement and fault length data for each New Zealand earthquake mainly plot along the upper bound, and above, the global data (Fig. 6b) and are sufficiently different to suggest that multi-fault ruptures of short faults cannot fully account for the differences in scaling relations between New Zealand and global datasets. Incomplete sampling of ruptured faults, particularly for pre-1930 earthquakes, could also partly account for the observed differences, as this would result in average displacement being a maximum and the total fault length a minimum. For example, inclusion of rupture on the Hikurangi interface in the 1855, 1931 and 2016 earthquakes would likely increase

18

the total lengths for these earthquake ruptures on Figure 6b. The inclusion of subsurface faults or faults that ruptured the ground surface, but were not identified, would tend to increase total lengths and push the New Zealand data further into the global dataset cloud.

Moment magnitude positively correlates with average displacement and length for New Zealand earthquakes (e.g., Fig. 6d). This correlation is expected as Mw is necessarily calculated for individual faults in multi-fault ruptures (i.e., all earthquakes except the 1888 North Canterbury Earthquake). Comparison of the New Zealand and global data suggests that for a given Mw average displacement is generally higher for the New Zealand faults (Fig. 6d), while lengths are generally shorter for New Zealand data. These observations support the view that New Zealand faults tend to be 'over displaced' and shorter than faults in the global compilation. As was the case in Figure 6b, summing lengths for each of the New Zealand earthquakes moves the New Zealand data into the data field for global earthquakes, which suggests that fault interactions and earthquake rupture across interconnected fault networks could partly account for the observed divergence between New Zealand and Global earthquake datasets (assuming that global data do not include a significant number of multi-fault events).

Factors controlling multi-fault ruptures

Historical earthquakes in New Zealand rupture interconnected fault networks, which are interpreted to favour multi-fault ruptures. These ruptures occur in a range of tectonic settings and across different fault types, with variable fault displacement rates. In some cases co-rupture of the Hikurangi subduction thrust (or thrust faults splaying from the subduction interface), may have facilitated (and linked) rupture of more than one fault (e.g., Wairarapa 1855, Hawkes Bay 1931 and Kaikōura 2016). For example, a blind thrust fault connects the northern (e.g., Kekerengu, Papatea and Upper Kowhai faults) and southern (e.g., Hundalee, Leader and The Humps faults) ruptures in the Kaikōura Earthquake, which are separated by at least 10 km at the surface. However, several of the historical multi-fault earthquakes in New Zealand (e.g., Buller 1929, Edgecumbe 1987 and Darfield 2010) are distal to the Hikurangi subduction thrust, which is unlikely to have contributed directly to the observed complexity of rupture geometries or to the rupture process. The common element for all multi-fault ruptures is the intersection or hard linkage of the constituent faults; presently there is no evidence to support the view that historical earthquakes in New Zealand jumped across unfaulted rock for distances of more than a few kilometres. This conclusion is consistent with 'jump-distance' data for strike-slip faults in California, which suggests that distances between co-rupturing faults at the ground surface are generally <5 km (Biasi and Wesnousky, 2016).

The number of fault intersections is likely to be impacted by the variability of fault strike and dip, and the density of faults. New Zealand appears to have a high density of mapped active faults compared to many other plate boundary regions, which might locally promote multi-fault ruptures. In New Zealand the 2021 Community Fault Model (CFM) comprises 880 active faults (Van Dissen et al., 2021; Seebeck et al., 2022) mapped over an area of ~400,000 km^2 (onshore and offshore) which is ~2.2 faults/1000 km^2. Whereas California has ~0.7 fault sections/1000 km^2 (i.e., 350 fault sections per ~500,000 km^2) and Taiwan ~1 fault/1000 km^2 (i.e., 40 mapped faults per ~40,000 km^2). The high density of active faults in New Zealand might partly reflect the high density of planes of weakness in basement rocks arising from >100 Myrs of episodic plate boundary deformation, the high rates of relative plate motion presently occurring across New Zealand (35-50 mm/yr) and the immaturity of our active fault systems (most active faults have <3 km of displacement). The rate dependence is illustrated by the apparent decrease in the densities of active faults with increasing distance from

the central high-strain rate zone of the New Zealand plate boundary (Stirling et al., 2012; Van Dissen et al., 2021).

Fault-network connections only provide part of the solution to what controls the occurrence of multi-fault ruptures. If fault geometry was the only determinant for rupture arrest, then a given network of faults would tend to rupture in characteristic earthquakes of similar size and repeated ruptures of the same set of faults. Static and dynamic stress models confirm that stresses acting of each fault strongly influence their ability to accrue slip during an earthquake (Stein et al., 1997; Stein, 1999; Richards-Dinger and Dieterich, 2012; Ando and Kaneko, 2018; Shaw et al 2022). If a fault is not well advanced in its seismic cycle and the static stresses on the fault plane too low, slip on an adjacent fault will not drive the fault to failure (Schwartz et al., 2012; Quigley et al., 2019). For example, the Hope Fault in the 2016 Kaikōura Earthquake may represent a geological example of the role of static stress and the stage of the seismic cycle on the fault. This fault accrued very little slip in 2016 despite carrying a relatively high slip rate of ~15-25 mm/yr (Langridge et al., 2003) and being surrounded by faults that ruptured in the Kaikōura Earthquake. Paleoseismic trenching suggests the fault has an average recurrence interval of ~200-400 yrs, however, the last two events on the fault may have occurred in quick succession (~40-180 years apart) with the last of these about 200 yrs ago (Hatem et al., 2019). These two most recent events may have de-stressed the fault and reset the seismic cycle clock meaning that future earthquakes may be delayed unless static and dynamic stresses during future earthquakes are sufficiently high to trigger slip (e.g., Ando and Kaneko, 2018).

The average displacement and length data may have important implications for the fundamental question "do multi-fault ruptures know how big they are going to be when they start?". We argue that if this were the case, then we would expect to see evidence of elevated average displacement or energy release on the nucleating fault. Instead, average displacement scales with length (Fig. 6) and gnerally does not appear to vary with position in the rupture sequence. This inference is consistent with observations from the Kaikōura Earthquake where the highest energy release and greatest average displacement occurred on the Upper Kowhai-Jordan-Kekerengu-Needles fault, the largest fault in the system that ruptured. Our data appear to support the view that the size of the rupture and its associated average displacement is mainly controlled by the dimensions of each fault surface and not by the faults position in multi-fault rupture sequence. By contrast, whether intersecting faults rupture together in the same earthquake is strongly influenced by their proximity, the static stresses acting on faults in the network, the dynamic stresses induced by the rupture process and possibly also by the strength properties of the faults at the time of rupture.

Frequency of multi-fault ruptures

For the purposes of understanding earthquake processes and seismic hazards it is important to consider how often multi-fault ruptures occur. The answer to this question may differ depending on whether we are considering the frequency of earthquakes of the same multi-fault earthquake or of any multi-fault earthquake in a fault system. In answer to the first question, it is clear that precisely the same multi-fault earthquake could occur infrequently (e.g., with recurrence intervals of thousands to tens of thousands of years). For example, Kaikōura Earthquake type events (i.e. earthquakes involving the specific faults that ruptured in 2016) can happen no more frequently than every ~3 kyr, which is approximately the recurrence interval of the lowest slip rate fault that ruptured in 2016. Similarly, because recurrence intervals on the Kekerengu Fault are hundreds of years in duration (mean 376 ± 32 years; Little et al., 2018), and about an order of magnitude shorter

than faults south of the Hope Fault (e.g., Brough et al., 2021), many of the earthquakes that rupture the Kekerengu Fault are unlikely to rupture the same faults south of the Hope Fault. For example, the recurrence interval on the Kekerengu Fault is only 10% that on The Humps Fault and, on average, at least 10 earthquakes would be required before co-rupture of these two faults is expected (Brough et al., 2021).

By contrast, it is possible that some of the faults that ruptured together in historical earthquakes always or often rupture together. For example, the Leader and Humps faults ruptured together in the Kaikōura Earthquake, with the Leader Fault accommodating oblique slip at the termination of the mainly strike-slip The Humps Fault (Nicol et al., 2018). The kinematic relationships of these faults are such that earthquakes nucleating on The Humps Fault could be terminated by slip on the Leader Fault. Support for this hypothesis is provided by the Mount Stewart Range, which is located at the eastern termination of The Humps Fault and has been interpreted to have formed due to oblique reverse displacement on the eastern Humps and Leader faults over million-year timescales. Similarly, the Papatea Fault may commonly rupture with the faults that it intersects (i.e., Kekerengu and Offshore Splay Thrust Fault). Support for this argument is provided by the estimated Mw of ~6.7 for rupture of the Papatea Fault on its own, which is below the ~Mw7 expected to produce surface rupture in New Zealand outside of the Taupo Rift (Nicol et al., 2016a).

Collectively the available literature for historical earthquakes in New Zealand and internationally supports the hypothesis that multi-fault ruptures are common (Beanland et al., 1989; Sieh et al., 1993; Kurushin et al., 1997; Schwartz et al., 2012; Grapes and Holgate, 2014; Fletcher et al., 2014; Page, 2020). Of the New Zealand historical earthquakes post 1840 at least five ruptured three or more faults (Wairarapa 1855, Hawkes Bay 1931, Edgecumbe 1987, Darfield 2010 and Kaikōura 2016 earthquakes). These observations suggest that single-fault ruptures are the exception rather than the rule with a high proportion of surface-rupturing earthquakes in New Zealand involving multi-fault ruptures. To rationalise the suggestion that large complex multi-fault earthquakes involving the same faults occur infrequently with the high frequency of multi-fault earthquakes in the historical record we propose that it must also be common for multi-fault ruptures in a given fault system to involve different faults. We propose that the main driver for these different fault-rupture patterns are changes in the static and dynamic stress regime.

Application of results to Seismic Hazard Assessment in New Zealand

Historical moderate to large magnitude earthquakes that ruptured the ground surface provide key input data for seismic hazard models (e.g., Smith and Berryman, 1986; Wells and Coppersmith, 1994; Stirling et al., 1998, 2002, 2012; Biasi and Weldon, 2006; Wesnousky, 2008; McCalpin, 2009; Biasi et al., 2013; Hecker et al., 2013; Field et al., 2014, 2015; Schwartz, 2018; Page 2020). Early seismic hazard models in New Zealand were constructed assuming that each fault or part of a fault (e.g., segment) ruptured separately from other faults in the system during earthquakes. The one-fault (or part-fault) one-earthquake approach that was generally adopted for earlier iterations on the NSHM was dictated by the computational limitations of the time. In the last 10 years historical earthquakes (e.g., Kaikōura 2016), the results from earthquake simulations and seismic hazard modelling highlight the prospect that multiple faults rupturing in the same earthquake (Richards-Dinger and Dieterich, 2012; Field et al., 2014; Hamling et al., 2017; Litchfield et al., 2018; Page, 2020; Shaw et al., 2022). Due in part to improvements in computational tools multi-fault ruptures were incorporated into version 3 of the 2015 Uniform California Earthquake Rupture Forecast (UCERF3)(Field et al., 2014, 2015) and, in a several cases, the 2010 NSHM (Stirling et al., 2012). The present 2022 iteration of the NSHM model has common elements to UCERF3 and will incorporate

multi-fault ruptures using Coulomb stress considerations to identify which faults could rupture together.

The present study informs the inclusion of multi-fault ruptures in future seismic hazard models. There is some debate in the literature about whether multi-fault ruptures are over-represented or under-represented in the UCERF3 model (Schwartz, 2018; Page, 2020) and the same discussion applies to the 2022 NSHM. This study suggests that most of our historical earthquakes were multi-fault ruptures and supports their inclusion in the NSHM at a level where they accommodate a significant proportion of the fault slip-rate budget. From the available historical earthquakes these multi-fault ruptures can extend at least several hundred kilometres along the plate boundary, although there are currently few constraints from the historical record on appropriate maximum lengths for these ruptures. The historical earthquake record does however support the view that shorter multi-fault ruptures and more frequent than longer ruptures. The record shows that multi-fault earthquakes with total rupture lengths of ≥100 km occur every ~35 years, rupture lengths of ≥280 km every 90 years and rupture lengths of >330 km >180 years. Although the data are sparse, these observations could be compared to model fault-rupture inversions from the 2022 NSHM to test their applicability to the available empirical data.

We can also cast light on the expected displacements on multi-fault ruptures compared to single fault events, which informs the average displacement and length scaling relations used for estimating average displacements and recurrence intervals when only fault-length data are available. Our data appears to show that the relationship between average displacement and length does not vary substantially for individual faults in multi-fault ruptures and individual faults in single fault ruptures. This similarity means that we can continue to use established displacement-length relationships from the literature to inform the scaling relations of multi-fault ruptures and supports the use of the scaling relations employed in the previous iteration of the NSHM (e.g., Stirling et al., 2012). However, if average displacements on individual faults are controlled by the dimensions of each individual fault surface (for which fault length is a proxy) and how it interacts with neighbouring faults, it can neither be used to determine how many faults ruptured in a given event (i.e., whether the displacement was generated by a multi-fault and single-fault earthquake), nor to argue for characteristic earthquakes.

Multi-fault ruptures can be expected to have a number of consequences for the quantification for earthquake parameters (compared to a one-fault one-earthquake model). First, a greater proportion of the total strain or slip budget will be taken up by larger earthquakes, which could result in a decrease of the b-value for an earthquake population. Second, multi-fault ruptures may lead to a decrease in the frequency of large magnitude earthquakes and to potential 'double counting' of some earthquakes in, for example, paleoseismic studies. Double counting will arise because the same earthquake could be identified as a separate earthquake on multiple faults. Thus, while trenching studies may correctly identify the number of slip events on a particular fault during the sample interval, they may over-estimate the number of primary earthquakes on a given fault (i.e., where the fault is the longest in the multi-fault rupture). Double counting in trenching studies could also lead to an over-estimate of the number of moderate to large magnitude earthquakes in a given region. The extent of this double counting is difficult to estimate as not all faults have been trenched and/or are incorporated into the NSHM. Of the faults that ruptured historical in the eight New Zealand earthquakes studied here, 14 are included in the 2021 CFM (Van Dissen et al., 2021; Seebeck et al., 2022), suggesting that on average ~1.8 faults (i.e. 14/8=1.75) in the model rupture together in multi-fault earthquakes. If this average applied across the entire CFM it would suggest that, on average, ~490 earthquakes would be required to rupture all 880 faults in the model.

A significant question remains as to whether the inclusion of multi-fault ruptures in seismic hazard models will significantly change the hazard. What seems likely is that multi-fault ruptures will produce larger earthquakes (i.e., greater magnitudes and total rupture lengths) and, to meet the seismic moment budget, possibly fewer smaller events moderate to large (e.g., < Mw 7) magnitude events. Despite a possible reduction in the number of large magnitude earthquakes the historical record for New Zealand suggest that they occur frequently. If, for example, all of the Mw >7 earthquakes in Table 1 except 1888 were multi-fault events then, on average, we can expect one large magnitude multi-fault event every 30 years. Given the high frequency of these earthquakes we propose that multi-fault earthquakes may generally increase hazard across New Zealand (because larger events occur more frequently). However, the precise change in hazard will depend on which faults rupture together, the proximity of the active faults to sites of interest and the time interval under consideration. Therefore, more work is required to examine the impact of multi-fault ruptures on seismic hazard both across New Zealand and at specific locations.

Conclusions

We have examined the geometries and displacements of eight historical moderate to great (Mw 6.4-8.2) surface-rupturing earthquakes in New Zealand since 1840 using the existing literature and reanalysis of surface ruptures. Our analysis indicates that at least five of these earthquakes ruptured three or more faults (Wairarapa 1855, Hawkes Bay 1931, Edgecumbe 1987, Darfield 2010 and Kaikōura 2016 earthquakes), while a further two earthquakes have been postulated to have ruptured multiple faults (Marlborough 1848 and Buller 1929). Therefore, historical rupture of multiple faults during individual earthquakes was the norm rather than the exception in New Zealand. These multi-fault ruptures occur for a range of fault types, with variable fault displacement rates and in different tectonic settings. The scaling relationships between average displacement and rupture length generally do not appear to vary between the largest (primary) and smaller (secondary) faults in an earthquake. These scaling relations are interpreted to be mainly controlled by the dimensions of each individual fault and not by the size of the earthquake or the total number of faults that it ruptures. Hard-linkage of individual faults in three-dimensions is observed for all historical multi-fault earthquakes. In the Wairarapa 1855, Hawkes Bay 1931 and Kaikōura 2016 earthquakes co-rupture of the Hikurangi subduction thrust (or thrust faults splaying from the subduction interface), may have facilitated (and linked) rupture of more than one fault. In other earthquakes multi-fault ruptures were far removed from subduction, which is unlikely to have directly contributed to the observed complexity of rupture geometries (e.g., Buller 1929, Edgecumbe 1987 and Darfield 2010). Fault interactions promoted by fault intersections and crustal stresses (both static and dynamic) are inferred to be the primary controls on the development of multi-fault ruptures. Multi-fault ruptures were included in the 2010 NSHM for some major faults, and are presently being substantially included in the 2022 NSHM. These multi-fault models are expected to increase the magnitudes and decrease the frequency of earthquakes of >Mw7 earthquakes relative to the earlier models. Further work is required to determine under what circumstances the inclusion of multi-fault ruptures in the New Zealand NSHM will increase overall seismic hazards.

Acknowledgements

References

Ando R, Kaneko Y. 2018. Dynamic rupture simulation reproduces spontaneous multifault rupture and arrest during the 2016 MW 7.9 Kaikōura earthquake. *Geophysical Research Letters* 45, 12,875–12,883, doi.org/10.1029/2018GL080550.

Bai YF, Lay T, Cheung KF, Ye LL. 2017. Two regions of seafloor deformation generated the tsunami for the 13 November 2016, Kaikōura, New Zealand earthquake. *Geophysical Research Letters* 44, 6597–6606 (2017).

Balfour, N.J.; Savage, M.K.; Townend, J. 2005. Stress and crustal anisotropy in Marlborough, New Zealand: evidence for low fault strength and structure-controlled anisotropy. *Geophysical Journal International* (2005) 163, 1073–1086, doi: 10.1111/j.1365-246X.2005.02783.x

Beanland, S., Berryman, K.R., Blick, G.H. 1989. Geological investigations of the 1987 Edgecumbe earthquake, New Zealand. *New Zealand Journal of Geology and Geophysics 32(1),* 73-91.

Beavan, J., Motagh, M., Fielding, E.J., Donnelly, N., Collett, D. 2012. Fault slip models of the 2010–2011 Canterbury, New Zealand, earthquakes from geodetic data and observations of postseismic ground deformation. *New Zealand Journal of Geology and Geophysics* 55(3), 207-221.

Beavan, J., Darby, D., 2005. Fault slip in the 1855 Wairarapa earthquake based on new and reassessed vertical motion observations: did slip occur on the sobduction interface? In: Townend, J., Langridge, R., Jones, A. (eds), The 1855 Wairarapa Earthquake Symposium. Greater Wellington Regional Council, Wellington, 31-41.

Begg, J.G., Johnston, M.R., (Compilers) 2000. Geology of the Wellington area. Institute of Geological and Nuclear Sciences 1:250 000 geological map 10, 1 sheet + 64p. Lower Hutt, New Zealand, Institute of Geological and Nuclear Sciences Limited.

Begg, J.G., Mouslopoulou, V., 2010. Analysis of late Holocene faulting within an active rift using lidar, Taupo Rift, New Zealand. *Journal of Volcanology and Geothermal Research* 190: 152-167, doi: 10.1016/j.jvolgeores.2009.06.001.

Berryman, K.R. 1980. Late Quaternary movement of the White Creek Fault, South Island, New Zealand. *New Zealand Journal of Geology and Geophysics* 23, 93-101.

Biasi, G.P., Weldon, R.J. 2006. Estimating Surface Rupture Length and Magnitude of Paleoearthquakes from Point Measurements of Rupture Displacement. *Bulletin of the Seismological Society of America* 96(5), 1612–1623, doi: 10.1785/0120040172.

Biasi, G.P., Parsons, T., Weldon, R.J., Dawson, T.E., 2013. Appendix J - Fault-to-fault rupture probabilities. Uniform California Earthquake Rupture Forecast, Version 3 (UCERF3)—The Time-Independent Model. USGS Open-File Report 2013-1165, CGS Special Report 228, and Southern California Earthquake Center Publication 1792.

Biasi, G. P., Wesnousky, S.G., 2016. Steps and gaps in ground ruptures: Empirical bounds on rupture propagation. *Bulletin of the Seismological Society of America* 106, 1110–1124.

Bilham, R., Bodin, P., 1992. Fault zone connectivity: slip rates and faults in the San Francisco Bay area, California. *Science* 258, 281–284.

Blick, G.H., Flaherty, M.P. 1989. Regional vertical deformation associated with the 1987 Edgecumbe earthquake, New Zealand. *New Zealand Journal of Geology and Geophysics* 32, 99-108.

Cesca, S., Zhang, Y., Mouslopoulou, V., Wang, R., Saul, J., Savage, M., Heimann, S., Kufner, S., Oncken, O., Dahm, T., 2017. Complex rupture process of the Mw 7.8, 2016, Kaikōura earthquake, New Zealand, and its aftershock sequence. *Earth and Planetary Science Letters* 478, 110-120.

Cowan, H.A. 1990. Late Quaternary displacements on the Hope Fault at Glyn Wye, North Canterbury. *New Zealand Journal of Geology and Geophysics* 33, 285-293.

Clark, K.J., Nissen, E.K., Howarth, J.D., Hamling, I.J., Mountjoy, J.J., Ries, W.F., Jones, K., Goldstien, S., Cochran, U.A., Villamor, P., Hreinsdóttir, S., Litchfield, N.J., Mueller, C., Berryman, K.R., Strong, D. T., 2017, Highly variable coastal deformation in the 2016 MW7.8 Kaikōura earthquake reflects rupture complexity along a transpressional plate boundary. *Earth and Planetary Science Letters* 474, 334-344.

Darby, D., 1987. Geodetic deformation analysis regionally for northern Hawkes Bay, and locally from the Mohaka River area. *New Zealand Geological Survey Report*, EDS 105, 1987.

Darby, D., Beanland, S., 1992. Possible source models for the 1855 Wairarapa Earthquake New Zealand. *Journal of Geophysical Research* 97(B9), 12,375-12,389.

Downes, G.L., Dowrick, D.J., 2014. Atlas of Isoseismal maps of New Zealand earthquakes, 1843-2003, 2nd Edition. *Institute of Geological & Nuclear Sciences monograph 25* (issued CD). Lower Hutt: Institute of Geological & Nuclear Sciences.

Edbrooke, S.W., Heron, D.W., Forsyth, P.J., Jongens, R., 2015. Geological map of New Zealand 1:1 000 000, GNS Science Geological Maps.

Elliott, J.R., Nissen, E.K., England, P.C., Jackson, J.A., Lamb, S., Li, Z., Oehlers, M., Parsons, B., 2012. Slip in the 2010 and 2011 Canterbury earthquakes, New Zealand. *Journal of Geophysical Research* 117, B03401, doi.org/10.1029/2011JB008868

Field, E. H., Arrowsmith, R.J., Biasi, G.P., Bird, P., Dawson, T.E., Felzer, K.R., Jackson, D.D., Johnson, K.M., Jordan, T.H., Madden, C., Michael, A.J., Milner, K.R., Page, M.T., Parsons, T., Powers, P.M., Shaw, B.E., Thatcher, W.R., Weldon II, R.J., Zeng, Y., 2014. Uniform California Earthquake Rupture Forecast, Version 3 (UCERF3) - The Time-Independent Model. *Bulletin of the Seismological Society of America* 104, 1122-1180.

Field, E.H., Biasi, G.P., Bird, P., Dawson, T.E., Felzer, K.R., Jackson, D.D., Johnson, K.M., Jordan, T.H., Madden, C., Michael, A.J., et al., 2015. Long-term time-dependent probabilities for the third Uniform California Earthquake Rupture Forecast (UCERF3). *Bulletin of the Seismological Society of America* 105, no. 2A, 511–543.

Fletcher, J.M., Teran, O.J., Rockwell, T.K., Oskin, M.E., Hudnut, K.W., Mueller, K.J., Spelz, R.M., Akciz, S.O.,. Masana, E., Faneros, G., Fielding, E.J., Leprince, S., Morelan, A.E., Stock, J., Lynch, D.K., Elliott, A.J., Gold, P., Liu-Zeng, J., González-Ortega, A. Hinojosa-Corona, A., González-García, J., 2014. Assembly of a large earthquake from a complex fault system: Surface rupture kinematics of the 4 April 2010 El Mayor-Cucapah (Mexico) M_w 7.2 earthquake. *Geosphere* 10, 797-827.

Fletcher, J., Oskin, M., Teran, O., 2016. The role of a keystone fault in triggering the complex El Mayor-Cucapah earthquake rupture. *Nature Geoscience* 9, 303-307, doi:10.1038/ngeo2660.

Furlong, K.P., Herman, M. 2017. Reconciling the deformational dichotomy of the 2016 Mw 7.8 Kaikoura NZ earthquake. *Geophysical Research Letters* 44, 6788–6791.

Grapes, R.H., Holdgate, G.R. 2014. Earthquake clustering and possible fault interactions across Cook Strait, New Zealand, during the 1848 and 1855 earthquakes. *New Zealand Journal of Geology and Geophysics*, doi: 10.1080/00288306.2014.907579.

Hamling, I.J., Hreinsdóttir, S., Clark, K., Elliott, J., Liang, C., Fielding, E., Litchfield, N., Villamor, P., Wallace, T., Wright, J. et al. 2017. Complex multifault rupture during the 2016 Mw 7.8 Kaikōura earthquake, New Zealand. *Science* 356: no. 6334.

Hamling, I.J, 2020. A review of the 2016 Kaikōura earthquake: insights from the first 3 years. *Journal of the Royal Society of New Zealand* 50(2), 226-244, doi: 10.1080/03036758.2019.1701048.

Hancox, GT, Ries WF, Parker, RN, Rosser BJ, 2015. Landslides caused by the Ms 78 Murchison Earthquake of 17 June 1929 in north west South Island, New Zealand, GNS Science Report 2015/42, Lower Hutt, New Zealand.

Hecker, S., Abrahamson, N.A., Wooddell, K.E., 2013. Variability of displacement at a point: implications for earthquake-size distribution and rupture hazard on faults. *Bulletin of the Seismological Society of America* 103(2A), 651–674, doi: 10.1785/0120120159.

Henderson, J. 1933. Geological aspects of the Hawke's Bay earthquakes. *New Zealand Journal of Science and Technology* 15, 38-75.

Henderson, J. 1937. The west Nelson earthquakes of 1929. *New Zealand Journal of Science and Technology* 19(2), 66-143.

Howell, A., Nissen, E., Stahl, T., Clark, K., Kearse, J., Van Dissen, R., Villamor, P., Langridge, R., Jones, K., 2020. Three-Dimensional Surface Displacements During the 2016 MW 7.8 Kaikōura Earthquake (New Zealand) From Photogrammetry-Derived Point Clouds. *Journal of Geophysical Research: Solid Earth* 125(1), p. e2019JB018739, https://doi .org/10.1029/2019JB018739.

Hull, A.G., 1990. Tectonics of the 1931 Hawke's Bay earthquake. *New Zealand Journal of Geology and Geophysics* 33(2), 309-320.

Humphrey, J., Nicol, A., 2020. Could the 1929 Ms7.8 Buller (Murchison) Earthquake have been a multi-fault rupture? In: Bassett K. N., Nichols A. R. L., Fenton C. H. eds. Geosciences 2020: Abstract Volume. Geoscience Society of New Zealand Miscellaneous Publication 157A. Geoscience Society of New Zealand, Wellington, pp. 139.

Ishibashi, K., 1987. Faulting of the 1931 Hawke's Bay earthquake and its implications in subduction tectonics in the Hikurangi Margin, North Island, New Zealand (preliminaries), in Holocene Coastal Tectonics of Eastern North Island, New Zealand, ed. Ota, Y., Dept. Geography, Yokohama National University, Japan, pp. 97–99.

Kearse, J., Little, T. A., Van Dissen, R. J., Barnes, P. M., Langridge, R., Mountjoy, J., Ries, W., Villamor, P., Clark, K. J., Benson, A., Lamarche, G., Hill, M., Hemphill-Haley, M., 2018, Onshore to Offshore Ground-Surface and Seabed Rupture of the Jordan–Kekerengu–Needles Fault Network during the 2016 Mw 7.8 Kaikōura Earthquake, New Zealand. *Bulletin of the Seismological Society of America* 108(3B), 1573-1595.

Kelsey, H.M., Hull, A.G., Cashman, S.M., Berryman, K.R., Cashman, P.H., Trexler, J.H., Begg, J.G. 1998. Paleoseismology of an active reverse fault in a forearc setting: the Poukawa fault zone, Hikurangi margin, New Zealand. *Geological Society of America Bulletin 110*, 1123-1148.

Khajavi, N., Langridge, R.M., Quigley, M.C., Smart, C., Rezanejad, A., Martín-González, F., 2016. Late Holocene rupture behavior and earthquake chronology on the Hope fault, New Zealand. *Geological Society of America Bull*etin B31199, 31191.

Khajavi, N., Nicol, A., Quigley, M., Langridge, R., 2018. Temporal slip-rate stability and variations on the Hope Fault, New Zealand, during the Late Quaternary. *Tectonophysics* 738, 112-123, doi.org/10.1016/j.tecto.2018.05.001.

Kurushin, R. A.,Bayasgalan,A., Ölziybat, M., Enkhtuvshin, B., Molnar, P., Bayarsayhan, C., Hudnut, K.W., Lin, J., 1997. The surface rupture of the 1957 Gobi-Altay, Mongolia, earthquake. *Geological Society of America Special Paper* 320, 143 pp.

Lajoie, L.J., Nissen, E., Johnson, K.L., Arrowsmith, J.R., Glennie, C.L., Hinojosa-Corona, A., Oskin, M.E., 2019, Extent of low-angle normal slip in the 2010 El Mayor-Cucapah (Mexico) earthquake from differential lidar. *Journal of Geophysical Research: Solid Earth* 124(1), 943-956.

Langridge, R.M., Campbell, J., Hill, N.L., Pere, V., Pope, J., Pettinga, J., Estrada, B., Berryman, K.R., 2003. Paleoseismology and slip rate of the Conway Segment of the Hope Fault at Greenburn Stream, South Island, New Zealand. *Annals of Geophysics* 46, 1119–1139.

Langridge, R.M., Ries, W.F., Litchfield, N.J., Villamor, P., Van Dissen, R.J., Barrell, D.J.A., Rattenbury, M.S., Heron, D.W., Haubrook, S., Townsend, D.B., et al., 2016. The New Zealand active faults database. *New Zealand. Journal of Geology and Geophysics* 59, 86–96.

Langridge, R.M., Rowland, J., Villamor, P., Mountjoy, J., Townsend, D.B., Nissen, E., Madugo, C., Ries, W.F., Gasston, C., Canva, A., Hatem, A.E., Hamling, I., 2018, Coseismic Rupture and Preliminary Slip Estimates for the Papatea Fault and Its Role in the 2016 Mw 7.8 Kaikōura, New Zealand, Earthquake. *Bulletin of the Seismological Society of America* 108(3B), 1596-1622.

Lee, J.M., Begg, J.G. (compilers) 2002: Geology of the Wairarapa area: scale 1:250,000. Lower Hutt: Institute of Geological & Nuclear Sciences Limited. Institute of Geological & Nuclear Sciences 1:250,000 geological map 11. 66 p. + 1 folded map

Lee, J.M., Townsend, D., Bland, K., Kamp, P.J.J. (compilers) 2011. Geology of the Hawke's Bay area: scale 1:250,000. Lower Hutt: Institute of Geological & Nuclear Sciences Limited. Institute of Geological & Nuclear Sciences 1:250,000 geological map 8. 86 p. + 1 folded map

Leonard, G.S., Begg, J.G., Wilson, C.J.J. (compilers) 2010. Geology of the Rotorua area: scale 1:250,000. Lower Hutt: Institute of Geological & Nuclear Sciences Limited. Institute of Geological & Nuclear Sciences 1:250,000 geological map 5. 99 p. + 1 folded map.

Litchfield, N., Van Dissen, R., Heron, D., Rhoades, D. 2006. Constraints on the timing of the three most recent surface rupture events and recurrence interval for the Ohariu Fault: trenching results from MacKays Crossing, Wellington, New Zealand. *New Zealand Journal of Geology and Geophysics* 49, 57–61.

Little, T.A., Van Dissen, R., Schermer, E., Carne, R. 2009. Late Holocene surface ruptures on the southern Wairarapa fault, New Zealand: Link between earthquakes and the uplifting of beach ridges on a rocky coast. *Lithosphere* 1, 4–19, doi:10.1130/L7.1.

McCalpin, J.P. (ed.) 2009. *Paleoseismology*, 2nd Edition: International Geophysics Series, Vol. 95, Elsevier Publishing, 647p.

Manighetti, I., Perrin, C, Dominguez, S., Garambois, S., Gaudemer, Y., Malavieille, J., Matteo, L., Delor, E., Vitard, C., Beauprêtre, S. 2015. Recovering paleoearthquake slip record in a highly dynamic alluvial and tectonic region (Hope Fault, New Zealand) from airborne lidar. *Journal of Geophysical Research Solid Earth*, 120, 4484–4509, doi:10.1002/2014JB011787.

Manighetti, I., Perrin, C., Gaudemer, Y., Dominguez, S., Stewart, N., Malavieille, J., Garambois, S., 2020. Repeated giant earthquakes on the Wairarapa fault, New Zealand, revealed by Lidar-based paleoseismology. *Scientific Reports 10:2124,* doi.org/10.1038/s41598-020-59229-3.

Mason, D.P.M, Little, T.A. 2006. Refined slip distribution and moment magnitude of the 1848 Marlborough earthquake, Awatere Fault, New Zealand. *New Zealand Journal of Geology and Geophysics* 49(3), 375-382, doi: 10.1080/00288306.2006.9515174.

Mouslopoulou, V., Nicol, A., Walsh, J.J., D. Beetham, D. Stagpoole, V. 2008. Quaternary temporal stability of a regional strike-slip fault and rift intersection. *Journal of Structural Geology* 30, 451-463.

Mouslopoulou V, Saltogianni V, Nicol A, Oncken O, Begg J, Babeyko A, Cesca S, Moreno M. 2019. Breaking a subduction-termination from top to bottom: the large 2016 Kaikōura Earthquake, New Zealand. *Earth and Planetary Science Letters* 506, 1-10.

Nathan, S., Rattenbury, M.S., Suggate, R.P. (compilers) 2002. Geology of the Greymouth area: scale 1:250,000. Lower Hutt: Institute of Geological & Nuclear Sciences. Institute of Geological & Nuclear Sciences 1:250,000 geological map 12. 58 p. + 1 folded map

Nicol, A., and Wise, D.U., 1992. Paleostress adjacent to the Alpine Fault of New Zealand: fault, vein and stylolite data from the Doctors Dome area. *Journal Geophysical Research* 97, 17,685-17,692.

Nicol, A., Walsh, J.J., Manzocchi, T., Morewood, N., 2005. Displacement rates and average earthquake recurrence intervals on normal faults. *Journal of Structural Geology* 27, 541-551.

Nicol, A., Walsh, J.J., Villamor, P., Seebeck, H., Berryman, K.R. 2010. Normal fault interactions, paleoearthquakes and growth in an active rift. *Journal of Structural Geology* 32, 1101-1113, doi:10.1016/j.jsg.2010.06.018.

Nicol A., Van Dissen, R., Stirling M., Gerstenberger, M., 2016a. Completeness of the paleoseismic active fault record in New Zealand. *Seismological Research Letters* 86 (6), 1299-1310, doi:10.1785/0220160088.

Nicol, A., Robinson, R., Van Dissen, R., Harvison, A., 2016b. Variability of recurrence interval and single-event slip for surface-rupturing earthquakes in New Zealand. *New Zealand Journal of Geology & Geophysics (Beavan volume)* 59, 97-116. DOI:10.1080/00288306.2015.1127822

Nicol, A., Khajavi, N., Pettinga, J.R., Fenton, C., Stahl, T., Bannister, S., Pedley, K., Hyland-Brook, N., Bushell, T., Hamling, I., Ristau, J., Noble, D., McColl, S.T., 2018, Preliminary Geometry, Displacement, and Kinematics of Fault Ruptures in the Epicentral Region of the 2016 Mw 7.8 Kaikōura, New Zealand, Earthquake. *Bulletin of the Seismological Society of America* 108(3B), 1521-1539.

Nicol, A., Begg, J., Saltogianni, V., Mouslopoulou, V., Oncken, O., Howell, A., 2022. Uplift and fault slip during the 2016 Kaikōura Earthquake and Late Quaternary, Kaikōura Peninsula, New Zealand. *New Zealand Journal of Geology and Geophysics: Kaikōura Earthquake Special Issue*, doi.org/10.1080/00288306.2021.2021955.

Page, M.T., 2020. More Fault Connectivity Is Needed in Seismic Hazard Analysis. *Bulletin of the Seismolological Society of America* 111, 391–397, doi: 10.1785/ 0120200119.

Quigley, M., Van Dissen, R., Litchfield, N., Villamor, P., Duffy, B., Barrell, D., Furlong, K., Stahl, T., Bilderback, E., Noble, D. 2012. Surface rupture during the 2010 Mw 7.1 Darfield (Canterbury) earthquake: implications for fault rupture dynamics and seismic-hazard analysis. *Geology* 40(1), 55-58, doi:10.1130/G32528.

Quigley, M.C., Jiménez, A., Duffy, B., King, T.R., 2019. Physical and statistical behavior of multifault earthquakes: Darfield earthquake case study, New Zealand. *Journal of Geophysical Research: Solid Earth 124*, doi.org/10.1029/2019JB017508

Rattenbury, M.S., Cooper, R.A., Johnston, M.R. (compilers), 1998. Geology of the Nelson area: scale 1:250,000. Lower Hutt: Institute of Geological & Nuclear Sciences Limited. Institute of Geological & Nuclear Sciences 1:250,000 geological map 9. 67 p. + 1 folded map.

Rattenbury, M.S., Townsend, D., Johnston, M.R. (compilers), 2006. Geology of the Kaikoura area: scale 1:250,000 geological map. Lower Hutt: GNS Science. Institute of Geological & Nuclear Sciences 1:250,000 geological map 13. 70 p. + 1 folded map

Richards-Dinger, K., Dieterich, J.H., 2012. RSQSim Earthquake Simulator. *Seismological Research Letters* 83, 983-990. doi:10.1785/0220120105. ISSN 0895-0695.

Rodgers, D.W., Little, T.A. 2006. World's largest coseismic strike-slip offset: The 1855 rupture of the Wairarapa Fault, New Zealand, and implications for displacement/length scaling of continental earthquakes. *Journal of Geophysical Research* 111, B12408, doi:10.1029/2005JB004065.

Satriano, C., Kiraly, E., Bernard, P., Vilotte, J.-P., 2012. The 2012 Mw 8.6 Sumatra earthquake: Evidence of westward sequential seismic ruptures associated to the reactivation of a N-S ocean fabric. *Geophysical Research Letters* 39(15), L15302, doi:10.1029/2012GL052387.

Schwartz, D.P., Coppersmith, K.J. 1984. Fault behavior and characteristic earthquakes: Examples from the Wasatch and San Andreas Fault zones. *Journal of Geophysical Research* 89, 5681–5698, doi:10.1029/JB089iB07p05681.

Schwartz, D.P., 2018. Review: Past and future fault rupture lengths in seismic source characterization - The long and short of it. *Bulletin of the Seismological Society of America,* doi:10.1785/0120160110.

Schwartz, D.P., Haeussler, P.J., Seitz, G.G., Dawson, T.E., 2012. Why the 2002 Denali fault rupture propagated onto the Totschunda fault: Implications for fault branching and seismic hazards. *Journal of Geophysical Research: Solid Earth* 117, no. B11.

Seebeck H, Van Dissen R, Litchfield N, Barnes P, Nicol A, Langridge R, Barrel D, Villamor P, Ellis S, Rattenbury M, et al., 2022 (in press). New Zealand Community Fault Model – version 1.0. Lower Hutt (NZ): GNS Science. (GNS Science report; 2021/57).

Shaw, B.E., Fry, B., Nicol, A., Howell, A., Gerstenberger, M.C., 2022. An earthquake simulator for New Zealand. *Bulletin of the Seismological Society of America,* doi: 10.1785/0120210087.

Sibson, R.H., Ghisetti, F.C., Ristau, J., 2011. Stress control of an evolving strike-slip fault system during the 2010–2011 Canterbury, New Zealand, earthquake sequence. *Seismological Research Letters* 82(6), 824–832.

Sieh, K., Jones, L., Hauksson, E., Hudnut, K., Eberhart-Phillips, D., Heaton, T., Hough, S., Hutton, K., Kanamori, H., Lilje, A., Lindvall, S., McGill, S. F., Mori, J., Rubin, C., Spotila, J. A., Stock, J., Thio, H.K., Treiman, J., Wernicke, B., and Zachariasen, J., 1993, Near-Field Investigations of the Landers Earthquake Sequence, April to July 1992. *Science*, 260(5105), 171-176.

Smith, W.D., Berryman, K.R., 1986. Earthquake hazard in New Zealand: Inferences from seismology and geology. In: *Recent crustal movements of the Pacific region.* Royal Society of New Zealand, Wellington. *Bulletin of the Royal Society of New Zealand* 24, 223-243.

Smith, E.G.C., Downes, G., 1997. Epicentres of large east coast North Island earthquakes, 1931–42, Research Report '97, School of Earth Sci., Victoria Univ. of Wellington, Wellington, New Zealand, 25–27.

Stein, R., Barka, A., Dieterich, J., 1997. Progressive failure on the North Anatolian Fault since 1939 by earthquake stress triggering. *Geophysical Journal International* 128, 594-604.

Stein, R., 1999. The Role of Stress Transfer in Earthquake Occurrence. *Nature* 402, 605-609.

Stirling, M.W., Wesnousky, S.G., Berryman, K.R., 1998. Probabilistic seismic hazard analysis of New Zealand. *New Zealand Journal Geology and Geophysics* 41, 355-375.

Stirling, M.W., McVerry, G.H., Berryman, K.R., 2002. A new seismic hazard model for New Zealand. *Bulletin of the Seismological Society of America* 92, 1878-1903.

Stirling, M., McVerry, G., Gerstenberger, M., Litchfield, N., Van Dissen, R., Berryman, K., Barnes, P., Wallace, L., Villamor, P., Langridge, R., Lamarche, G., Nodder, S., Reyners, M., Bradley, B., Rhodes, D., Smith, W., Nicol, A., Pettinga, J., Clark, K., Jacobs, K., 2012. National Seismic Hazard Model for New Zealand: 2010 Update. *Bulletin of the Seismological Society of America* 102(4), 1514-1542, doi: 10.1785/0120110170.

Stirling, M., Goded, T., Berryman, K., Litchfield, N., 2013. Selection of earthquake scaling relationships for seismic hazard analysis. *Bulletin of the Seismological Society of America* 103(6) 2993-3011, doi: 10.1785/0120130052.

Townend, J., Sherburn, S., Arnold, R., Boese, C., Woods, L., 2012. Three-dimensional variations in present-day tectonic stress along the Australia–Pacific plate boundary in New Zealand. *Earth and Planetary Science Letters*, *353*, 47-59, doi: 10.1016/j.epsl.2012.08.003.

Van Dissen, R., Yeats, R.S., 1991. Hope fault, Jordan thrust, and uplift of the seaward Kaikoura Range, New Zealand. *Geology* 19, 393-396.

Van Dissen, R., Seebeck, H., Litchfield, N., Barnes, P., Nicol, A., Langridge, R., Barrell, D., Villamor, P., et al. 2021. Development of the New Zealand Community Fault Model – version 1.0. *Proceedings of the 2021 New Zealand Society for Earthquake Engineering Annual Technical Conference.* https://repo.nzsee.org.nz/handle/nzsee/2366.

Villamor, P., Van Dissen, R.J., Alloway, B.V., Palmer, A.S., Litchfield, N.J., 2007. The Rangipo Fault, Taupo rift, New Zealand: an example of temporal slip-rate and single-event displacement variability in a volcanic environment. *Bulletin of the Geological Society of America* 119, 529–547.

Walcott, R.I., 1978. Geodetic strains and large earthquakes in the axial tectonic belt of North Island, New Zealand. *Journal of Geophysical Research* 83, 4419–4429.

Wells, D.L., Coppersmith, K.J., 1994. New empirical relationships among magnitude, rupture length, rupture width, rupture area, and surface displacement. *Bulletin of the Seismological Society of America* 84, 974-1002.

Wesnousky, S.G., 2008. Displacement and geometrical characteristics of earthquake surface ruptures: Issues and implications for seismic hazard analysis and the process of earthquake rupture. *Bulletin of the Seismological Society of America* 98(4), 1609–1632, doi: 10.1785/0120070111.

Yue, L.-F., Suppe, J., Hung, J.-H., 2005, Structural geology of a classic thrust belt earthquake: the 1999 Chi-Chi earthquake Taiwan (Mw=7.6). *Journal of Structural Geology* 27(11), 2058-2083.

Zinke, R., Hollingsworth, J., Dolan, J.F., Van Dissen, R., 2019. Three-dimensional surface deformation in the 2016 MW 7.8 Kaikōura, New Zealand, earthquake from optical image correlation: Implications for strain localization and long-term evolution of the Pacific- Australian plate boundary. *Geochemistry, Geophysics, Geosystems* 20, 1609–1628, doi.org/10.1029/2018GC007951.

Appendix 1 Rupture maps

Figure A1. Marlborough 1848 Mw 7.6 surface rupture map. Fault traces modified from Grapes and Holgate (2014). Cloudy Bay Fault is inferred to connect the Awatere and Ohariu/Wellington faults. Epicentre location nominally located at the coast. CBF = Cloudy Bay Fault, VF = Vernon Fault.
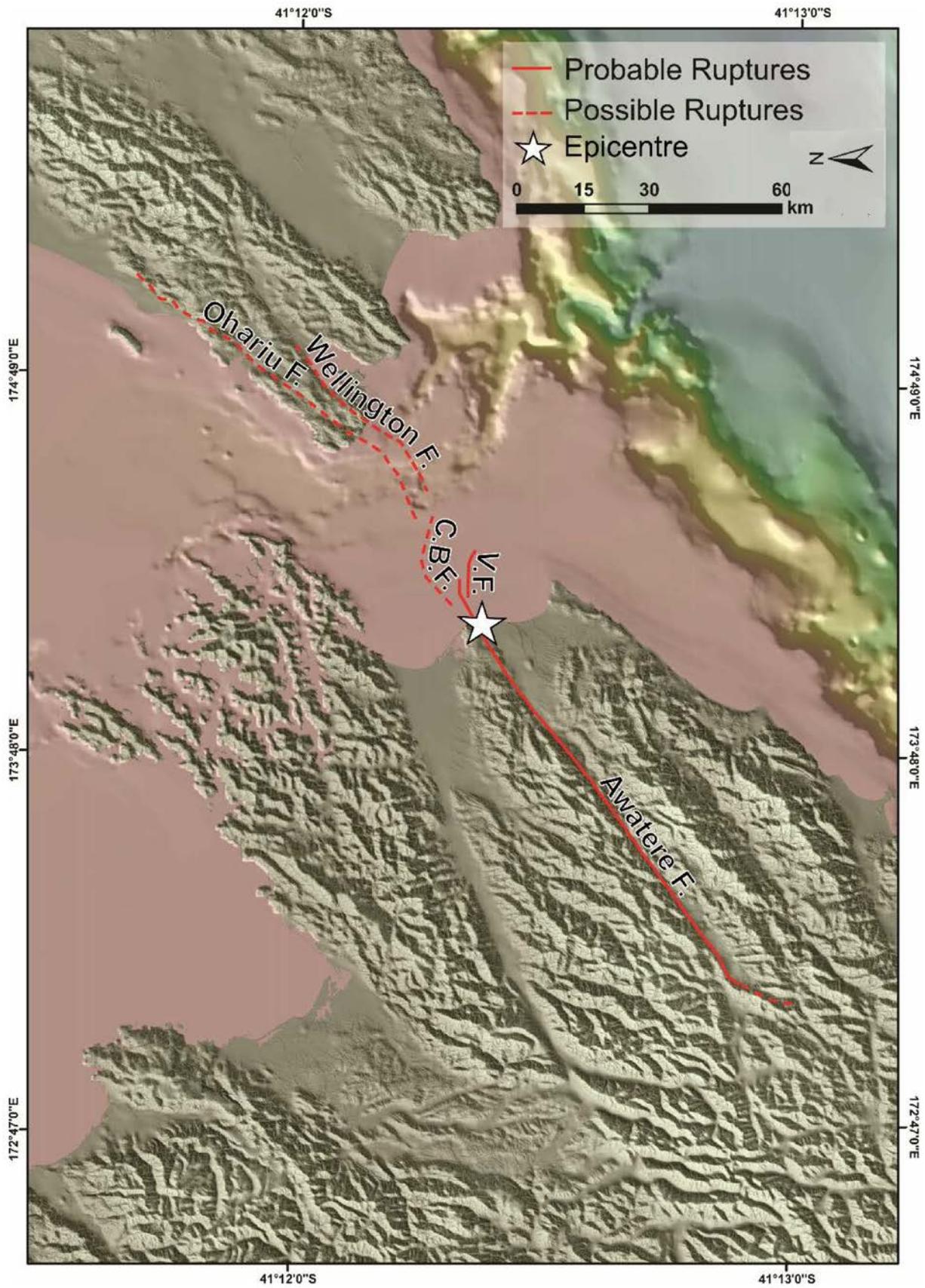
Figure A2. Wairarapa Earthquake 1855 Mw 8.2 surface-rupture map. Fault traces modified from Grapes and Holgate (2014). Epicentre located at the centre of isoseismals from Downes and Dowrick (2014). This generic epicentre location does not recognize that the Wairarapa Fault dips west (Darby and Beanland 1992). A number of publications indicate that rupture probably started up to 30 km west of surface rupture on the Wairarapa Fault possibly well on the Hikurangi plate interface at a depth of ~25 km west of the fault (Darby and Beanland 1992; Grapes and Downes 1997).
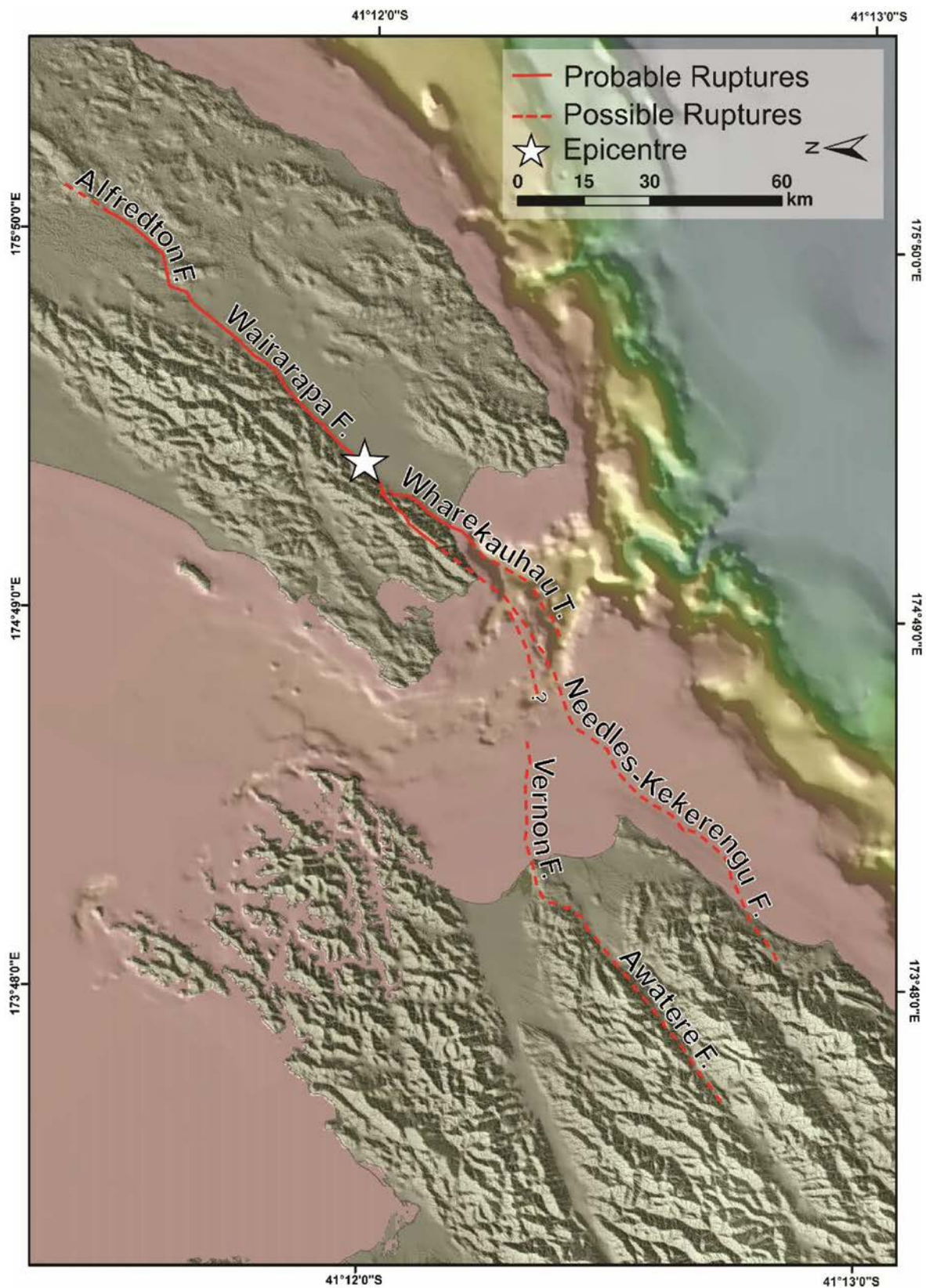
Figure A3. North Canterbury Earthquake 1888 Mw 7.1 surface rupture map. Epicentre Downes and Dowrick 2014 (42.6°S, 172.55°E), but moved north from Kakapo Fault on to trace of Hope Fault. Traces modified from Khajavi et al. (2014).
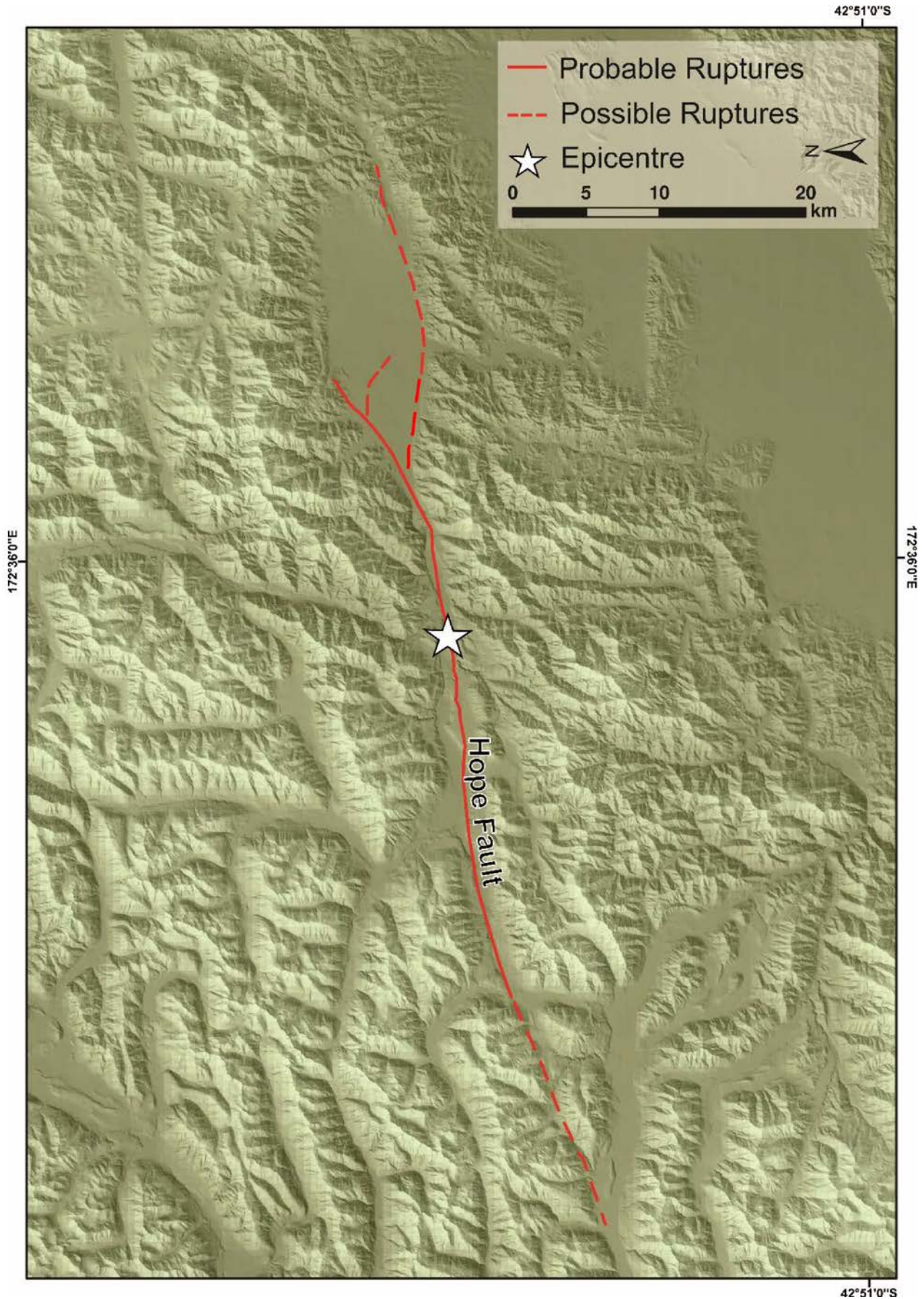
Figure A4. Buller 1929 Mw 7.7 surface rupture map. Rupture traces from Humphrey and Nicol (2020). Epicentre location modified from Downes and Dowrick 2014 (41.7°S, 172.2°E) assuming a focal depth of 20 km and a fault dip of 60°. WCF= Whale Creek Fault, GF= Glengarry Fault, LF= Longford Fault (representative for flexural slip planes in Longford Syncline).
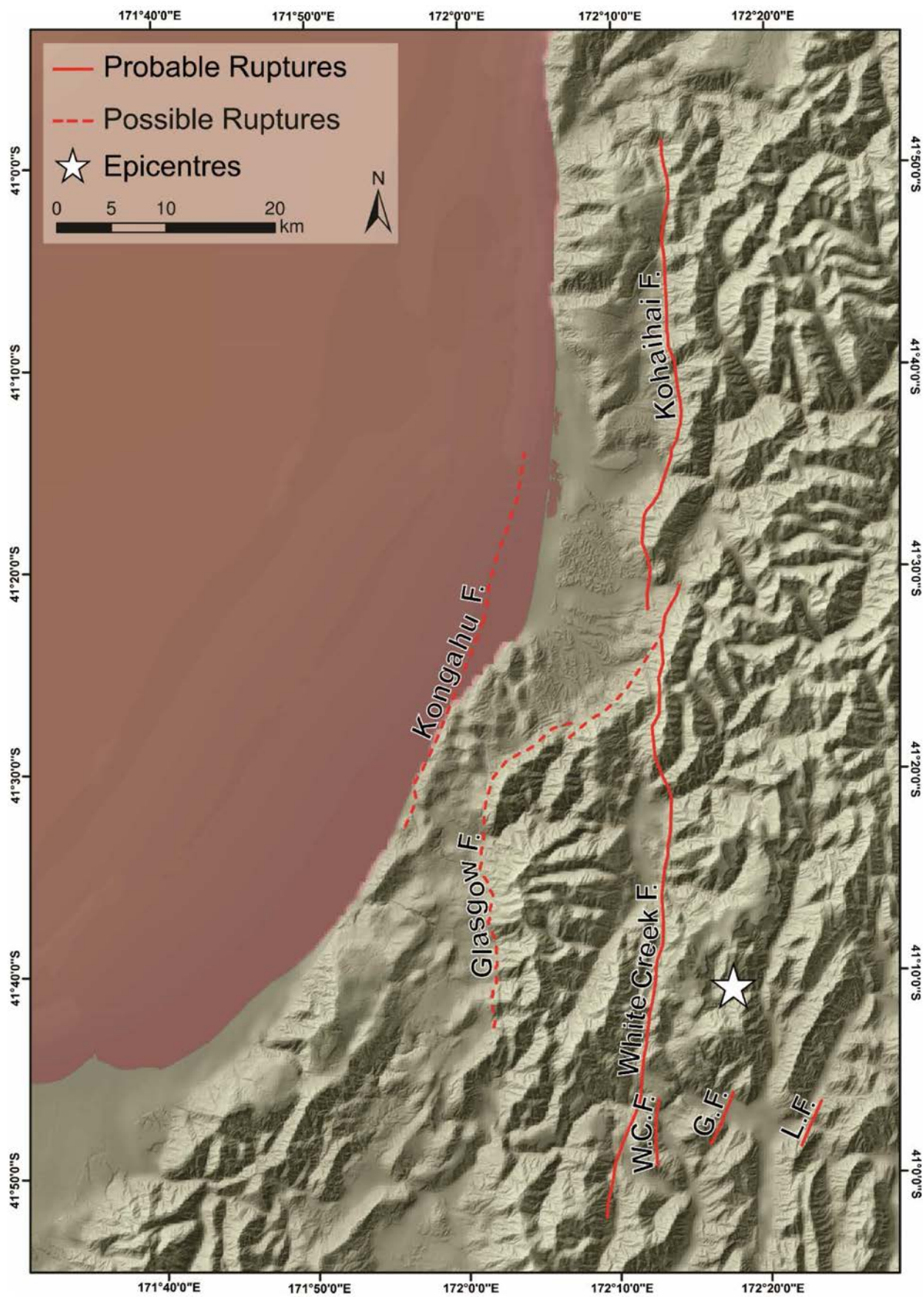
Figure A5. Hawkes Bay Earthquake 1931 Mw 7.8 surface rupture map. Onshore fault traces interpreted from lidar (this study) with reference to Hull (1990) and Kelsey et al. (1998). Fault names from Langridge et al. (2016). Epicentre location from Smith and Downes (1997) (39.69°S, 176.73°E) and does not take account of the focal depth or the dip of the Napier Fault (~40°).
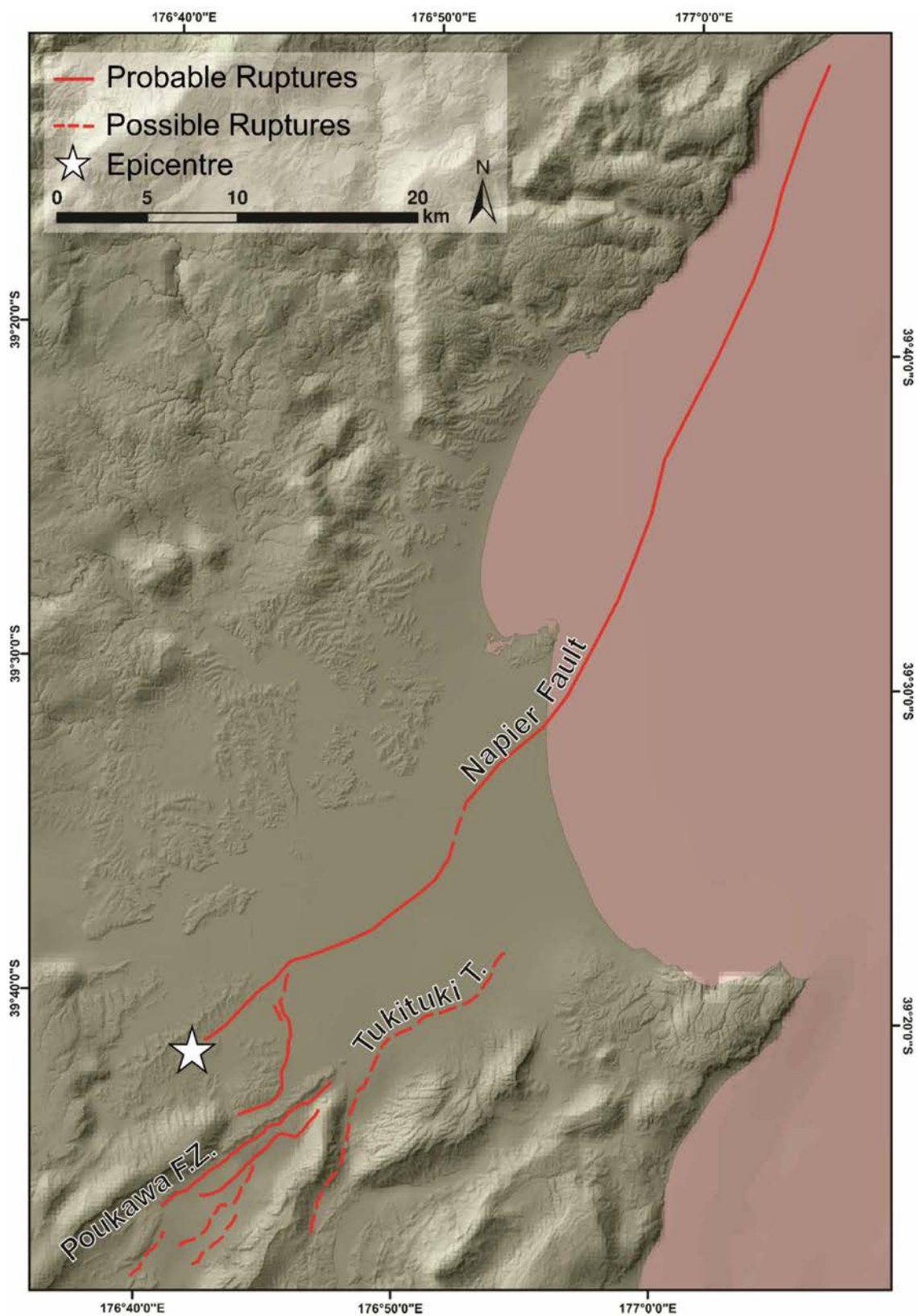

Figure A6. Edgecumbe Earthquake 1987 Mw 6.4 surface-rupture map. Onshore fault traces interpreted from lidar (this study) with reference to Beanland et al. (1989). Fault names from Langridge et al. (2016). Epicentre location from Downes and Dowrick 2014 (37.89°S, 176.80°E).
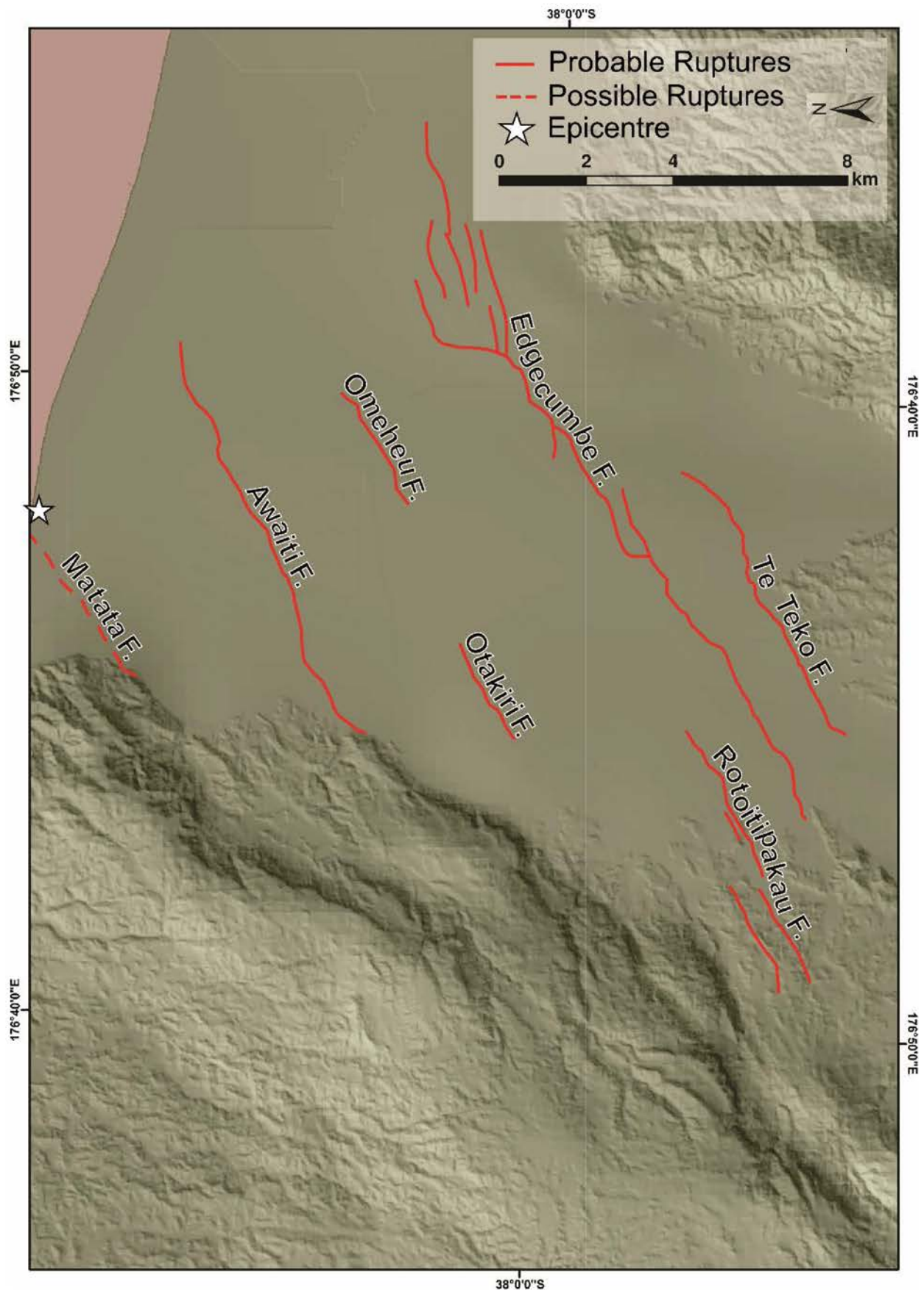
Figure A7. Darfield Earthquake 2010 Mw 7.1 surface rupture map. Fault locations from Quigley et al., (2012) and Beavan et al. (2012). HAF= Hororata Fault, GFW= Greendale Fault West, GFC=

Greendale Fault Central, GFE= Greendale Fault East, CCF= Charing Cross Fault, CCFN= Charing Cross Fault North, SKF= Sandy Knolls Fault. Epicentre location from Geonet (43.53°S, 172.17°E); Retrieved April 21st 2022.
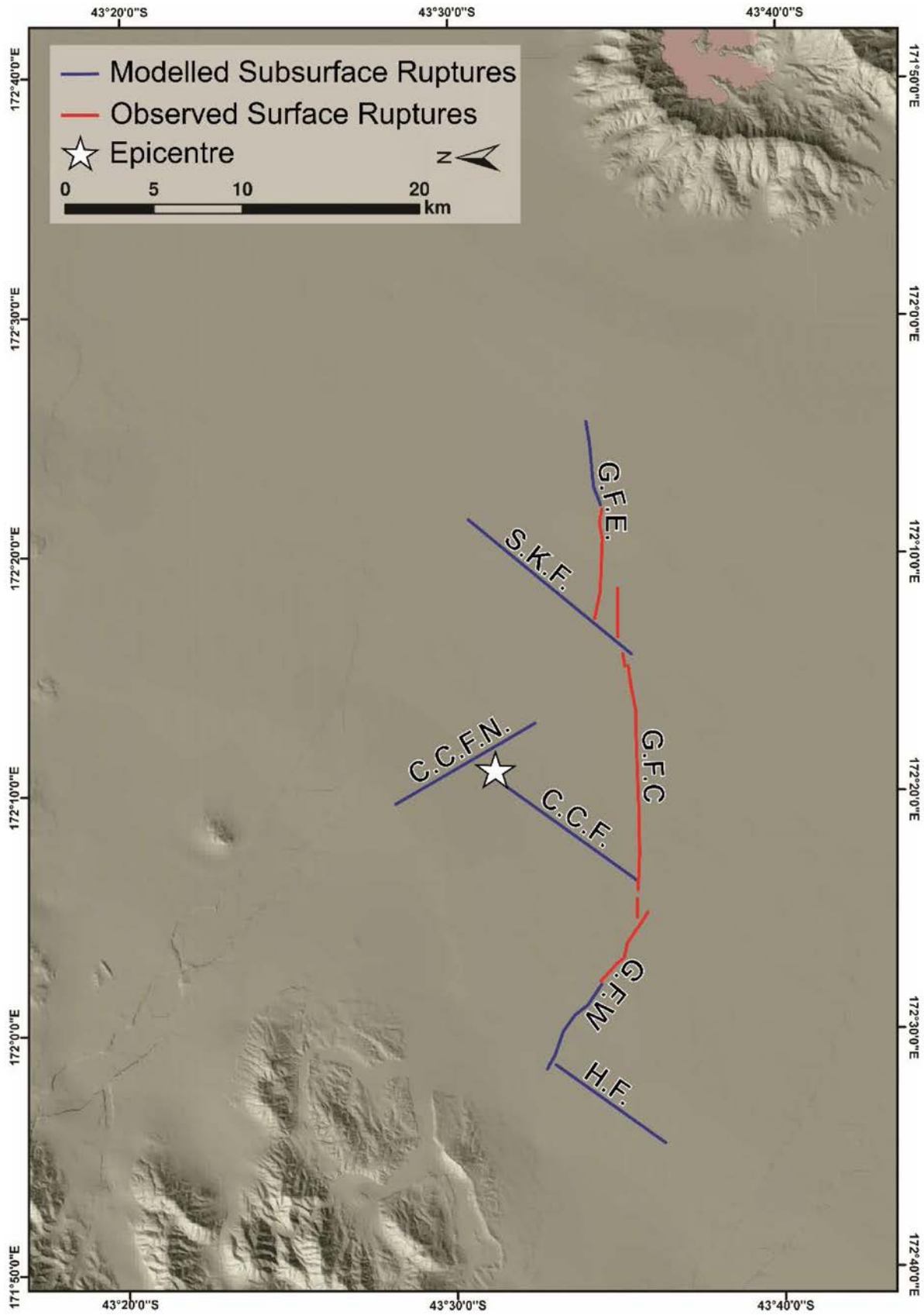
Figure A8. Kiakōura Earthquake 2016 Mw 7.8 surface-rupture map. Fault traces modified from Litchfield et al. (2018). Epicentre location from Nicol et al. 2018 (42.656°S, 172.982°S). THF= The Humps Fault, LF= Leader Fault, SJF= Stone Jug Fault, HF= Hundalee Fault, HoF= Hope Fault, PKF= Point Kean Fault, OSTF= Offshore Thrust Fault, FF= Fidget Fault, PF= Papatea Fault, UKF= Upper Kowai Fault, KF= Kekerengu Fault, NF= Needles Fault.
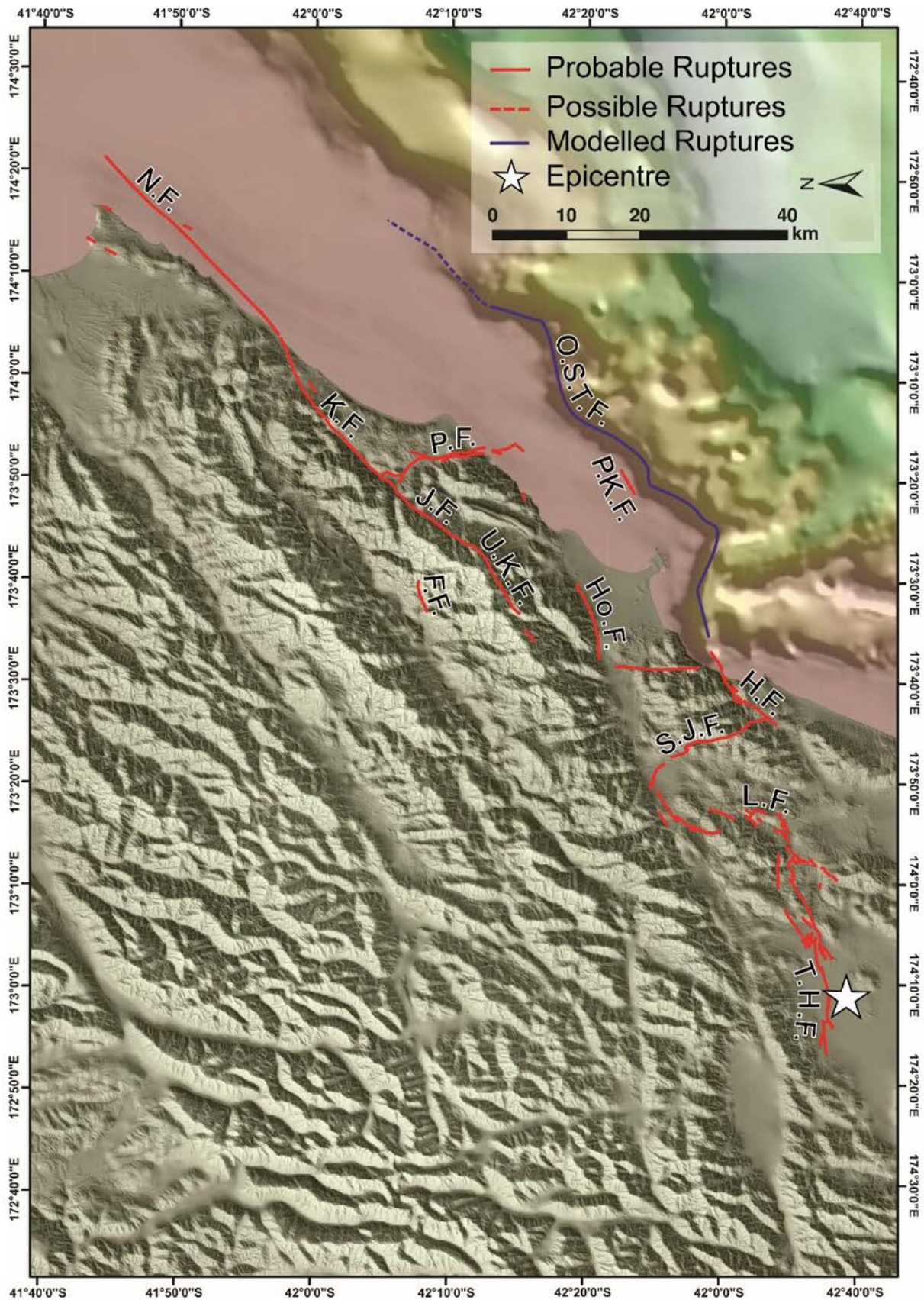
Appendix 2 Outputs and End users

Conferences

Nicol, A., Van Dissen, R.J., Stirling, M.W., Gerstenberger, M.C., Khajavi, N., 2017. Large magnitude earthquakes in New Zealand: what is the norm? Seismological Society of America Annual Meeting Denver 15-21 2017. Seismological Research Letters 88, No. 2B, 678.

Khajavi, N, Nicol, A., Fenton, C., Pettinga, J., Stahl, T., Hyland, N., Bushell, T., Pedley, K., McColl, S., Noble, D. 2017. Preliminary geometry and kinematics of multiple surface ruptures during the 2016 M_W 7.8 Kaikōura earthquake, North Canterbury region, New Zealand. Proceedings of the 8th International INQUA Meeting on Paleoseismology, Active Tectonics and Archeoseismology. Handbook and Programme, 13-16 November 2017, Blenheim, New Zealand. Lower Hutt (NZ): GNS Science. 441 p. (GNS Science miscellaneous series 110). doi:10.21420/G2H061.

Bushell, T., Nicol, A., Fenton, C., Khajavi, N., Hyland, N., Pettinga, J., Stahl, T. 2017. Fault rupture patterns during the Mw7. 8 2016 Kaikōura Earthquake in the region between the Leader and Charwell rivers, north Canterbury, New Zealand. Proceedings of the 8th International INQUA Meeting on Paleoseismology, Active Tectonics and Archeoseismology. Handbook and Programme, 13-16 November 2017, Blenheim, New Zealand. Lower Hutt (NZ): GNS Science. 441 p. (GNS Science miscellaneous series 110). doi:10.21420/G2H061.

Hyland N., Nicol A., Fenton CH., Khajavi N., Pettinga J., Bushell T. 2017. Preliminary insights into the fault geometries and kinematics of surface rupture along the South Leader Fault. Proceedings of the 8th International INQUA Meeting on Paleoseismology, Active Tectonics and Archeoseismology. Handbook and Programme, 13-16 November 2017, Blenheim, New Zealand. Lower Hutt (NZ): GNS Science, 441 p. (GNS Science miscellaneous series 110). doi:10.21420/G2H061. http://www.earthquakegeology.com/materials/proceedings/2017_Blenheim.pdf

Nicol, A., Van Dissen, R.J., Stirling, M.W., Gerstenberger, M.C., Khajavi, N., 2017. Large magnitude earthquakes and seismic hazard in New Zealand. 2017 Taiwan-Japan-New Zealand seismic hazard assessment meeting, 30 Oct. 2017 – 03 Nov. 2017, National Cheng Kung University, Tainan, Taiwan.

Nicol, A., Khajavi, N., Kearse, J., Van Dissen, R.J., Stirling, M.W., Gerstenberger, M.C., 2018. How important are multi-fault ruptures in New Zealand earthquakes. In: Sagar M, Prebble J ed. Abstract Volume: Geosciences 2018, Napier, New Zealand. Geoscience Society of New Zealand Miscellaneous Publication 151A. p 197.

Nicol, A., Khajavi, N., Kearse, J., Van Dissen, R.J., Stirling, M.W., Gerstenberger, M.C., 2018. Multi-fault ruptures during New Zealand historical earthquakes and seismic hazard assessment. 2018 Taiwan-Japan-New Zealand seismic hazard assessment meeting, 12 Nov. 2018 – 18 Nov. 2018, Oamaru, New Zealand.*?*

Humphrey, J., Nicol, A., 2020. Could the 1929 Ms7.8 Buller (Murchison) Earthquake have been a multi-fault rupture? In: Bassett K. N., Nichols A. R. L., Fenton C. H. eds. Geosciences 2020: Abstract Volume. Geoscience Society of New Zealand Miscellaneous Publication 157A. Geoscience Society of New Zealand, Wellington, pp. 139.

Theses

Brough, T., 2019. Tectonic Geomorphology and Paleoseismology of The Humps Fault Zone, North Culverden Basin. MSc thesis, University of Canterbury, 93 p.

Scott, B., 2019. The Stone Jug Fault: Facilitating Sinistral Displacement Transfer During the Mw7.8 Kaikōura Earthquake. MSc thesis, University of Canterbury, 112 p.

Papers

Nicol, A., Khajavi, N., Pettinga, J. R., Fenton, C., Stahl, T., Bannister, S., Pedley, K., Hyland-Brook, N., Bushell, T., Hamling, I., Ristau, J., Noble, D., and McColl, S. T., 2018, Preliminary Geometry, Displacement, and Kinematics of Fault Ruptures in the Epicentral Region of the 2016 Mw 7.8 Kaikōura, New Zealand, Earthquake: Bulletin of the Seismological Society of America, v. 108, no. 3B, p. 1521-1539.

Litchfield N., Villamor P., Van Dissen R., Nicol A., Barnes P., Barrell D., Pettinga J., Langridge R., Little T., Mountjoy J. Ries, W.F., Rowland, J., Fenton, C., Stirling, M.W., Kearse, J., Cochran, U.A., Clark, K.J., Hemphill-Haley, M., Khajavi, N., Jones, K., Archibald, G., Upton, P., Asher, C., Benson, A., Cox, S.C., Gasston, C., Hale, D., Hall, B., Hatem, A.E., Heron, D.W., Howarth J., Kane, T.J., Lamarche, G., Lawson, S., Lukovic, B., McColl, S.T., Madugo, C., Manousakis, J., Noble, D., Pedley, K., Sauer, K., Stahl, T., Strong, D.T., Townsend, D.B., Toy, V., Williams, J., Woelz, S., Zinke, R. 2018. Surface Fault Rupture from the Mw 7.8 2016 Kaikōura Earthquake, New Zealand, and Insights into Factors Controlling Multi-Fault Ruptures. *Bulletin of the Seismological Society of America* 108 (3B), 1496-1520. https://doi.org/10.1785/0120170300

Nicol, A., Begg, J., Saltogianni, V., Mouslopoulou, V., Oncken, O., Howell, A., 2022. Uplift and fault slip during the 2016 Kaikōura Earthquake and Late Quaternary, Kaikōura Peninsula, New Zealand. New Zealand Journal of Geology and Geophysics: Kaikōura Earthquake Special Issue, https://doi.org/10.1080/00288306.2021.2021955.